Molecular Biology of the Cell
Vol. 19, 1783–1797, April 2008

Protein Kinases Fpk1p and Fpk2p are Novel Regulators of Phospholipid Asymmetry

Kenzi Nakano,* Takaharu Yamamoto,† Takuma Kishimoto,* Takehiro Noji,* and Kazuma Tanaka†

Division of Molecular Interaction, Institute for Genetic Medicine, Hokkaido University Graduate Schools of *Medicine and †Life Science, Sapporo 060-0815, Japan

Submitted July 9, 2007; Revised December 20, 2007; Accepted January 8, 2008
Monitoring Editor: Sandra Lemmon

Type 4 P-type ATPases (flippases) are implicated in the generation of phospholipid asymmetry in membranes by the inward translocation of phospholipids. In budding yeast, the *DRS2*/*DNF* family members Lem3p-Dnf1p/Dnf2p and Cdc50p-Drs2p are putative flippases that are localized, respectively, to the plasma membrane and endosomal/*trans*-Golgi network (TGN) compartments. Herein, we identified a protein kinase gene, *FPK1*, as a mutation that exhibited synthetic lethality with the *cdc50*Δ mutation. The kinase domain of Fpk1p exhibits high homology to plant phototropins and the fungus *Neurospora crassa* NRC-2, both of which have membrane-associated functions. Simultaneous disruption of *FPK1* and its homolog *FPK2* phenocopied the *lem3*Δ/*dnf1*Δ *dnf2*Δ mutants, exhibiting the impaired NBD-labeled phospholipid uptake, defects in the early endosome-to-TGN pathway in the absence of *CDC50*, and hyperpolarized bud growth after exposure of phosphatidylethanolamine at the bud tip. The *fpk1*Δ *fpk2*Δ mutation did not affect the subcellular localization of Lem3p-Dnf1p or Lem3p-Dnf2p. Further, the purified glutathione *S*-transferase (GST)-fused kinase domain of Fpk1p phosphorylated immunoprecipitated Dnf1p and Dnf2p to a greater extent than Drs2p. We propose that Fpk1p/Fpk2p are upstream activating protein kinases for Lem3p-Dnf1p/Dnf2p.

INTRODUCTION

Despite experimental uncertainties concerning the distribution of lipids in organelle membranes, it is widely accepted that eukaryotic cell membranes have asymmetric lipid distribution. This phospholipid asymmetry has been most well characterized in the plasma membrane. In general, the aminophospholipids phosphatidylserine (PS) and phosphatidylethanolamine (PE) are enriched in the inner leaflet facing the cytoplasm, whereas phosphatidylcholine (PC), sphingomyelin, and glycolipids are predominantly found in the outer leaflet of the plasma membrane (Devaux, 1991; Zachowski, 1993; Pomorski *et al.*, 2001). Phospholipid asymmetry is generated and maintained by ATP-driven lipid transporters or translocases. The type 4 subfamily of P-type ATPases (also called "flippases") is implicated in the translocation of phospholipids from the external to the cytosolic leaflet (Graham, 2004; Pomorski *et al.*, 2004; Holthuis and Levine, 2005; Devaux *et al.*, 2006; Daleke, 2007). Five members of this subfamily (Drs2p, Neo1p, Dnf1p, Dnf2p, and Dnf3p) are encoded in the genome of the yeast *Saccharomyces cerevisiae* (Catty *et al.*, 1997).

Though no type 4 P-type ATPase has been shown to exhibit phospholipid translocase activity in reconstitution experiments with purified enzymes and chemically defined vesicles, accumulating evidence suggests that the yeast ATPases possess this activity in membranes. Dnf1p and Dnf2p are localized to the plasma membrane, and loss of Dnf1p and Dnf2p abolishes ATP-dependent transport of fluorescent 7-nitrobenz-2-oxa-1,3-diazol-4-yl (NBD)-labeled analogues of PE, PS, and PC from the outer to the inner plasma membrane leaflet (Pomorski *et al.*, 2003). Chemical labeling of outer-leaflet phospholipids and staining with a PE-specific probe showed that PE is exposed on the outer leaflet in *dnf1*Δ *dnf2*Δ mutant cells (Pomorski *et al.*, 2003; Iwamoto *et al.*, 2004). Drs2p is localized to endosomes and the *trans*-Golgi network (TGN), and Drs2p-dependent NBD-phospholipid translocase activity has been detected in Golgi membranes (Natarajan *et al.*, 2004) and post-Golgi secretory vesicles (Alder-Baerens *et al.*, 2006). In such vesicles, Drs2p was required for the asymmetric arrangement of PE (Alder-Baerens *et al.*, 2006).

Our recent results suggest that the Drs2p and Dnf1p/Dnf2p/Dnf3p proteins form complexes with members of the conserved Lem3p-Cdc50p family of membrane proteins. Cdc50p, Lem3p, and Crf1p were coimmunoprecipitated with Drs2p, Dnf1p and Dnf2p, and Dnf3p, respectively, and these proteins were required for the endoplasmic reticulum (ER) exit of the P-type ATPases (Saito *et al.*, 2004; Furuta *et al.*, 2007). Although we should await purification of the native proteins to conclude that these putative phospholipid translocases except for Neo1p are composed of noncatalytic and catalytic subunits, their heteromeric nature is reminis-

This article was published online ahead of print in *MBC in Press* (http://www.molbiolcell.org/cgi/doi/10.1091/mbc.E07–07–0646) on January 16, 2008.

Address correspondence to: Kazuma Tanaka (k-tanaka@igm.hokudai.ac.jp).

Abbreviations used: DIC, differential interference contrast; GFP, green fluorescent protein; mRFP1, monomeric red fluorescent protein 1; 3HA, three tandem repeats of the influenza virus hemagglutinin epitope; GST, glutathione *S*-transferase; NBD, 7-nitrobenz-2-oxa-1,3-diazol-4-yl; NBD-PC, 1-palmitoyl-2-(6-NBD-aminocaproyl)-PC; NBD-PE, 1-palmitoyl-2-(6-NBD-aminocaproyl)-PE; NBD-PS, 1-palmitoyl-2-(6-NBD-aminocaproyl)-PS; PE, phosphatidylethanolamine; PC, phosphatidylcholine; PS, phosphatidylserine; TGN, *trans*-Golgi network.

cent of the α-β subunit composition of the well-characterized P-type ATPase, Na^+,K^+-ATPase (Kaplan, 2002). It is currently unknown whether the Cdc50p family possesses regulatory function after the complex has reached its destination (e.g., the plasma membrane for Lem3p-Dnf1p; Noji *et al.*, 2006).

These putative heteromeric flippases are essential for cell growth, with Cdc50p-Drs2p, Lem3p-Dnf1p/Dnf2p, and Crf1p-Dnf3p playing major, intermediate, and minor roles, respectively (Hua *et al.*, 2002; Saito *et al.*, 2004). Recent studies suggest that Cdc50p-Drs2p and Lem3p-Dnf1p are not stably associated with their primary localization sites; both Cdc50p-Drs2p and Lem3p-Dnf1p are recycled from the plasma membrane through early endosomes to the TGN and back to the plasma membrane (Saito *et al.*, 2004; Liu *et al.*, 2007). This overlapping localization may underlie the functional redundancy between Cdc50p-Drs2p and Lem3p-Dnf1p/Dnf2p. Combined mutation of these genes compromises vesicle transport pathways, including endocytic internalization at low temperatures (*dnf1*Δ *dnf2*Δ *drs2*Δ; Pomorski *et al.*, 2003), vacuolar transport of alkaline phosphatase from the TGN (*drs2*Δ *dnf1*Δ; Hua *et al.*, 2002), and transport from early endosomes to the TGN (*cdc50 lem3*Δ *crf1*Δ; Furuta *et al.*, 2007).

One important approach toward understanding the physiological significance of phospholipid asymmetry would be identification of the regulatory pathways signaling to flippases and exploration of the upstream signals that they receive. We have recently shown that Cdc50p-Drs2p interacts with Rcy1p, a potential effector of the Rab family small GTPases Ypt31p/32p (Chen *et al.*, 2005), and have proposed that the Ypt31p/32p-Rcy1p pathway regulates Cdc50p-Drs2p to promote the formation of transport vesicles destined for the TGN from early endosomes (Furuta *et al.*, 2007). Because Lem3p-Dnf1p/Dnf2p are involved in the endocytic recycling pathway in conjunction with Cdc50p-Drs2p (Furuta *et al.*, 2007), it might be expected that Lem3p-Dnf1p and Lem3p-Dnf2p would be regulated by the Ypt31p/32p-Rcy1p pathway. However, neither Dnf1p nor Dnf2p interacts with Rcy1p (Furuta *et al.*, 2007), suggesting that Lem3p-Dnf1p/Dnf2p are regulated in a different manner.

In this study, we identify a protein kinase gene, *FPK1*, in our collection of mutations that exhibited synthetic lethality with *cdc50*Δ (Kishimoto *et al.*, 2005). Our results suggest that Fpk1p and its homologue Fpk2p are upstream regulatory protein kinases for Lem3p-Dnf1p and Lem3p-Dnf2p.

MATERIALS AND METHODS

Media and Genetic Methods

Strains were cultured in YPDA rich medium (1% yeast extract [Difco Laboratories, Detroit, MI], 2% bacto-peptone [Difco], 2% glucose, and 0.01% adenine). Strains carrying plasmids were selected in synthetic medium (SD) containing the required nutritional supplements (Rose *et al.*, 1990). Synthetic complete medium (SC) was SD medium containing all required nutritional supplements. When appropriate, 0.5% casamino acids (Difco) were added to SD medium without uracil (SDA-Ura). For induction of the *GAL1* promoter, 3% galactose and 0.2% sucrose were used as carbon sources instead of glucose (YPGA and SGA-Ura). Growth sensitivity to duramycin was examined on YPDA plates containing 5 μM duramycin (Sigma, St. Louis, MO). Standard genetic manipulations of yeast were performed as described previously (Guthrie and Fink, 1991).

Escherichia coli strains DH5α and XL1-Blue were used for construction and amplification of plasmids. The lithium acetate method was used to introduce plasmids into yeast cells (Elble, 1992; Gietz and Woods, 2002).

Strains and Plasmids

Yeast strains used in this study are listed in Table 1. Yeast strains carrying complete gene deletions (*fpk1*Δ and *fpk2*Δ), green fluorescent protein (GFP)-tagged genes (*KEX2*, *MYO2*, *DNF1*, and *DNF2*), monomeric red fluorescent protein 1 (mRFP1)-tagged *SEC7*, three tandem repeats of the influenza virus hemagglutinin epitope (3HA)-tagged genes (*DNF1* and *DNF2*), and 13 × myc-tagged genes (*DNF1*, *DNF2*, *DNF3*, *DRS2*, and *NEO1*) were constructed by PCR-based procedures as described (Longtine *et al.*, 1998; Goldstein and McCusker, 1999). The *GAL1* promoter-inducible C-terminal *FPK1* fragment (amino acids 445-893) tagged with glutathione *S*-transferase (P_{GAL1}-*GST-FPK1*Δ*N*) was similarly constructed. All strains constructed by PCR-based procedures were verified by colony-PCR amplification to confirm that the replacement had occurred at the expected locus.

The plasmids used in this study are listed in Table 2. The *FPK1(K525R)* allele was generated using a QuikChange site-directed mutagenesis kit (Stratagene, La Jolla, CA) with pKT1631 (YCplac111-FPK1). We sequenced the entire open reading frame of *FPK1(K525R)* to verify that only the desired substitutions were introduced. Schemes detailing the construction of plasmids and DNA sequences of nucleotide primers are available on request.

Isolation of New Mutants Synthetically Lethal with the *cdc50*Δ Mutation

Mutants synthetically lethal with *cdc50*Δ were newly isolated according to procedures described previously (Kishimoto *et al.*, 2005). Single recessive mutations were identified by genetic analyses, and the corresponding wild-type genes were cloned. For nonessential genes, null mutations were confirmed to be synthetically lethal with *cdc50*Δ. For essential genes, identity was confirmed by tetrad analysis with marker-tagged wild-type or temperature-sensitive alleles (our unpublished results).

Microscopic Observations

Most GFP- or mRFP1-tagged proteins were observed in living cells, which were grown to early-midlogarithmic phase, harvested, and resuspended in SC medium. Cells were mounted on microslide glass and immediately observed. Localization of GFP-Tlg1p and mRFP1-Snc1p was examined in fixed cells. Fixation was performed by addition of a commercial 37% formaldehyde stock (Wako Pure Chemicals, Osaka, Japan) into the medium to a final concentration of 0.5%, followed by a 10-min incubation at 30°C. After fixation, cells were washed twice with phosphate-buffered saline (PBS) and examined.

Endosomal structures were visualized by brief labeling with the lipophilic styryl dye FM4-64 (Invitrogen, Carlsbad, CA). Cells were grown to early-logarithmic phase in YPDA medium at 30°C for 3 h. Four OD_{600} units of cells were labeled with 32 μM FM4-64 in 100 μl of YPDA medium for 30 min on ice. Cells were harvested by centrifugation, resuspended in 200 μl of fresh YPDA medium, and incubated at 30°C for 1 min. Cells were washed twice with 100 μl of ice-cold SC medium and immediately observed using a G-2A filter set. The vacuole lumen was visualized using Cell Tracker Blue CMAC (Invitrogen) according to the manufacturer's protocol.

Cells were observed using a Nikon ECLIPSE E800 microscope (Nikon Instec, Tokyo, Japan) equipped with an HB-10103AF super high pressure mercury lamp and a 1.4 NA 100× Plan Apo oil immersion objective (Nikon Instec) with the appropriate fluorescence filter sets (Nikon Instec) and differential interference contrast (DIC) optics. Images were acquired with a digital cooled charge-coupled device camera (C4742–95-12NR; Hamamatsu Photonics, Hamamatsu, Japan) using AQUACOSMOS software (Hamamatsu Photonics). Observations are compiled from the examination of at least 100 cells.

Ultrastructural observation of cells by conventional electron microscopy was performed using the glutaraldehyde-osmium fixation technique according to procedures described previously (Sakane *et al.*, 2006).

Staining of Phosphatidylethanolamine with Biotinylated Ro09-0198 Peptide

PE staining in the outer leaflet of the plasma membrane was performed with biotinylated Ro09-0198 peptide (Bio-Ro) as described (Iwamoto *et al.*, 2004) with the following modifications. Bio-Ro was prepared essentially as described (Aoki *et al.*, 1994). A 1-ml culture of cells (midlogarithmic phase, generally at a cell density of 0.4–0.6 OD_{600}/ml) was harvested, resuspended in 20 μl of YPDA containing 100 μM Bio-Ro (for wild type), 30 μM (for *lem3*Δ), or 15 μM (for *fpk1*Δ *fpk2*Δ), and incubated for 13 h (for wild type and *fpk1*Δ *fpk2*Δ) or 15 min (for *lem3*Δ) on ice. The cells were washed once with PBS and fixed with 5% formaldehyde in PBS for 1 h at room temperature. After two washes with spheroplast buffer (1.2 M sorbitol, 0.1 M potassium phosphate, pH 7.4), cells were resuspended in 100 μl of spheroplast buffer containing 100 μg/ml zymolyase 100T (Seikagaku Kogyo, Tokyo, Japan) and 2.2 mg/ml β-mercaptoethanol (Wako Pure Chemicals) and incubated for 10 min at 30°C. After two washes with spheroplast buffer, spheroplast cells were attached to poly-L-lysine–coated multiwell slides, fixed in methanol and acetone, and incubated in PBS containing 0.1% bovine serum albumin (Sigma) for 20 min at room temperature. To visualize Bio-Ro, cells were washed three times with PBS and incubated in PBS containing 5 μg/ml fluorescein streptavidin (Vector Laboratories, Burlingame, CA) for 1 h at room temperature. After five washes with PBS, cells were stained with 4′ 6-diamidino-2-phenylindole (DAPI), suspended in 90% glycerol containing *n*-propyl gallate, and observed using an FITC (for fluorescein) bandpass or a UV-1A filter set.

Table 1. Yeast strains used in this study

Strain[a]	Relevant genotype	Derivation/source
BY4743	*MAT***a**/α *LYS2/lys2Δ0 ura3Δ0/ura3Δ0 his3Δ1/his3Δ1 leu2Δ0/leu2Δ0 met15Δ0/MET15*	Brachmann *et al*. (1998)
YEF473	*MAT***a**/α *lys2–810/lys2–810 ura3–52/ura3–52 his3Δ-200/his3Δ-200 trp1Δ-63/trp1Δ-63 leu2Δ-1/leu2Δ-1*	Longtine *et al*. (1998)
KKT33	*MAT***a** *lys2Δ0 ura3Δ0 his3Δ1 leu2Δ0 met15Δ0 DNF1-GFP::HIS3MX6*	This study
KKT39	*MAT***a** *lys2Δ0 ura3Δ0 his3Δ1 leu2Δ0 met15Δ0 DNF1-3HA::HIS3MX6*	This study
KKT58	*MATα lys2Δ0 ura3Δ0 his3Δ1 leu2Δ0 met15Δ0 KEX2-GFP::HIS3MX6*	This study
KKT61	*MAT***a** *LYS2 ura3Δ0 his3Δ1 leu2Δ0 MET15*	This study
KKT62	*MAT***a** *lys2Δ0 ura3Δ0 his3Δ1 leu2Δ0 met15Δ0 SEC7-mRFP1::HIS3MX6*	This study
KKT70	*MATα LYS2 ura3Δ0 his3Δ1 leu2Δ0 MET15*	This study
KKT72	*MATα LYS2 ura3Δ0 his3Δ1 leu2Δ0 MET15 fpk1Δ::HphMX4*	This study
KKT75	*MATα lys2Δ0 ura3Δ0 his3Δ1 leu2Δ0 MET15 MYO2-GFP::HIS3MX6*	This study
KKT102	*MAT***a** *LYS2 ura3Δ0 his3Δ1 leu2Δ0 met15Δ0 lem3Δ::KanMX6*	This study
KKT117	*MATα lys2Δ0 ura3Δ0 his3Δ1 leu2Δ0 MET15 HphMX4::P_{GAL1}-3HA-CDC50 fpk1Δ::KanMX6*	This study
KKT127	*MATα LYS2 ura3Δ0 his3Δ1 leu2Δ0 met15Δ0 HphMX4::P_{GAL1}-3HA-CDC50*	Sakane *et al*. (2006)
KKT266	*MAT***a** *LYS2 ura3Δ0 his3Δ1 leu2Δ0 MET15 fpk2Δ::KanMX6*	This study
KKT268	*MAT***a** *LYS2 ura3Δ0 his3Δ1 leu2Δ0 MET15 fpk1Δ::HphMX4 fpk2Δ::KanMX6*	This study
KKT287	*MAT***a** *LYS2 ura3Δ0 his3Δ1 leu2Δ0 MET15 HphMX4::P_{GAL1}-3HA-CDC50*	This study
KKT293	*MAT***a** *LYS2 ura3Δ0 his3Δ1 leu2Δ0 met15Δ0 HphMX4::P_{GAL1}-3HA-CDC50 lem3Δ::KanMX6*	This study
KKT330	*MAT***a** *LYS2 ura3Δ0 his3Δ1 leu2Δ0 MET15 HIS3MX6::P_{GAL1}-3HA-CDC50 fpk1Δ::HphMX4 fpk2Δ::KanMX6*	This study
KKT331	*MAT***a** *LYS2 ura3Δ0 his3Δ1 leu2Δ0 MET15 HIS3MX6::P_{GAL1}-3HA-CDC50 fpk2Δ::KanMX6*	This study
KKT332	*MAT***a** *lys2Δ0 ura3Δ0 his3Δ1 leu2Δ0 met15Δ0 DNF1-GFP::HIS3MX6 fpk1Δ::HphMX4 fpk2Δ::KanMX6*	This study
KKT334	*MAT***a** *LYS2 ura3Δ0 his3Δ1 leu2Δ0 MET15 DNF2-GFP::HIS3MX6*	This study
KKT336	*MAT***a** *LYS2 ura3Δ0 his3Δ1 leu2Δ0 MET15 DNF2-GFP::HIS3MX6 fpk1Δ::HphMX4 fpk2Δ::KanMX6*	This study
KKT340	*MAT***a** *LYS2 ura3Δ0 his3Δ1 leu2Δ0 MET15 DNF1–3HA::HIS3MX6 fpk1Δ::HphMX4 fpk2Δ::KanMX6*	This study
KKT342	*MAT***a** *LYS2 ura3Δ0 his3Δ1 leu2Δ0 MET15 DNF2–3HA::HIS3MX6*	This study
KKT344	*MAT***a** *LYS2 ura3Δ0 his3Δ1 leu2Δ0 MET15 DNF2–3HA::HIS3MX6 fpk1Δ::HphMX4 fpk2Δ::KanMX6*	This study
KKT345	*MATα LYS2 ura3Δ0 his3Δ1 leu2Δ0 MET15 HIS3MX6::P_{GAL1}-GST-FPK1ΔN*	This study
KKT346	*MAT***a** *LYS2 ura3Δ0 his3Δ1 leu2Δ0 met15Δ0 KEX2-GFP::HIS3MX6 lem3Δ::KanMX6*	This study
KKT347	*MAT***a** *LYS2 ura3Δ0 his3Δ1 leu2Δ0 met15Δ0 KEX2-GFP::HIS3MX6 HphMX4::P_{GAL1}-3HA-CDC50*	This study
KKT348	*MAT***a** *LYS2 ura3Δ0 his3Δ1 leu2Δ0 met15Δ0 KEX2-GFP::HIS3MX6 HphMX4::P_{GAL1}-3HA-CDC50 lem3Δ::KanMX6*	This study
KKT349	*MAT***a** *LYS2 ura3Δ0 his3Δ1 leu2Δ0 MET15 KEX2-GFP::HIS3MX6 HIS3MX6::P_{GAL1}-3HA-CDC50 fpk1Δ::HphMX4 fpk2Δ::KanMX6*	This study
KKT350	*MAT***a** *LYS2 ura3Δ0 his3Δ1 leu2Δ0 MET15 KEX2-GFP::HIS3MX6 fpk1Δ::HphMX4 fpk2Δ::KanMX6*	This study
KKT351	*MAT***a** *LYS2 ura3Δ0 his3Δ1 leu2Δ0 met15Δ0 MYO2-GFP::HIS3MX6 lem3Δ::KanMX6*	This study
KKT353	*MAT***a** *lys2Δ0 ura3Δ0 his3Δ1 leu2Δ0 MET15 MYO2-GFP::HIS3MX6 fpk1Δ::HphMX4 fpk2Δ::KanMX6*	This study
YKT1363	*MATα lys2-810 ura3-52 his3Δ-200 trp1Δ-63 leu2Δ-1 DNF1-13myc::TRP1 fpk1Δ::HphMX4 fpk2Δ::KanMX6*	This study
YKT1364	*MATα lys2-810 ura3-52 his3Δ-200 trp1Δ-63 leu2Δ-1 DNF2-13myc::TRP1 fpk1Δ::HphMX4 fpk2Δ::KanMX6*	This study
YKT1365	*MATα lys2-810 ura3-52 his3Δ-200 trp1Δ-63 leu2Δ-1 DNF3-13myc::TRP1 fpk1Δ::HphMX4 fpk2Δ::KanMX6*	This study
YKT1366	*MATα lys2-810 ura3-52 his3Δ-200 trp1Δ-63 leu2Δ-1 DRS2-13myc::TRP1 fpk1Δ::HphMX4 fpk2Δ::KanMX6*	This study
YKT1367	*MATα lys2-810 ura3-52 his3Δ-200 trp1Δ-63 leu2Δ-1 NEO1-13myc::TRP1 fpk1Δ::HphMX4 fpk2Δ::KanMX6*	This study

[a] KKT strains are isogenic derivatives of BY4743. YKT strains are isogenic derivatives of YEF473.

Internalization of Fluorescence-labeled Phospholipids into Yeast Cells

Large unilamellar vesicles containing NBD-phospholipids were prepared as described (Saito *et al.*, 2004). 1-Palmitoyl-2-(6-NBD-aminocaproyl)-PE (NBD-PE), 1-palmitoyl-2-(6-NBD-aminocaproyl)-PC (NBD-PC), 1-palmitoyl-2-(6-NBD-aminocaproyl)-PS (NBD-PS), and dioleoylphosphatidylcholine (DOPC) were obtained from Avanti Polar Lipids (Alabaster, AL). Fluorescently labeled phospholipid internalization experiments were performed as described previously (Kato *et al.*, 2002; Saito *et al.*, 2004). Briefly, cells were grown to early-midlogarithmic phase in YPDA media at 30°C. After dilution to 0.35 OD_{600}/ml in SC medium, cells were shaken for 30 min at 30°C with vesicles containing 40% NBD-phospholipids and 60% DOPC at a final concentration of 50 μM. Cells were then suspended in SC medium containing 0.01% NaN_3 and 2.5 μg/ml propidium iodide (PI) to allow the exclusion of PI-positive dead cells in flow cytometric analysis. Flow cytometry of NBD-labeled cells was performed on a FACS Calibur cytometer using the CellQuest software (BD Biosciences, San Jose, CA). NBD green fluorescence was plotted on a histogram to allow calculation of the mean fluorescence intensity.

Efflux of Phospholipids from Yeast Cells

Fluorescently labeled phospholipid efflux experiments were performed as described by Hanson and Nichols (2001). Cells were labeled with NBD-phospholipids for 60 min at 30°C as described above. To achieve equal levels of fluorescence in the strains to be compared, the concentration of an NBD-lipid for loading was adjusted according to the capability of each strain for the uptake of NBD-phospholipid. For the uptake of NBD-PE, the *lem3*Δ mutant was incubated at 50 μM, whereas the wild type and the *fpk1*Δ *fpk2*Δ mutant were incubated at 2.5 and 3 μM, respectively. For NBD-PS, the *fpk1*Δ *fpk2*Δ mutant was incubated at 50 μM, whereas the wild type and the *lem3*Δ mutant were incubated at 5 and 2 μM, respectively. After labeling, the cells were washed three times with ice-cold SC medium, resuspended in SC medium, and incubated at 30°C. At the given time

Table 2. Plasmids used in this study

Plasmid	Characteristics	Derivation/source
YCplac111	*LEU2 CEN4*	Gietz and Sugino (1988)
YEplac181	*LEU2 2 μm*	Gietz and Sugino (1988)
YEplac195	*URA3 2 μm*	Gietz and Sugino (1988)
pKO10	P_{GAL1}*-HA URA3 2 μm*	Kikyo *et al.* (1999)
pRS416-GFP-SNC1 pm	P_{TPI1}*-GFP-SNC1 pm URA3 CEN6*	Lewis *et al.* (2000)
pKT1340 [YEplac181-LEM3]	*LEM3 LEU2 2 μm*	Noji *et al.* (2006)
pKT1563 [pRS416-mRFP1-SNC1]	P_{TPI1}*-mRFP1-SNC1 URA3 CEN6*	Furuta *et al.* (2007)
pKT1566 [YEplac181-GFP-TLG1]	*GFP-TLG1 LEU2 2 μm*	Furuta *et al.* (2007)
pKT1602 [YEplac195-DNF1]	*DNF1 URA3 2 μm*	Noji *et al.* (2006)
pKT1631 [YCplac111-FPK1]	*FPK1 LEU2 CEN4*	This study
pKT1632 [YEplac195-FPK1]	*FPK1 URA3 2 μm*	This study
pKT1633 [YCplac111-FPK1(K525R)]	*FPK1(K525R) LEU2 CEN4*	This study
pKT1634 [pRS416-GFP-FPK1]	P_{FPK1}*-GFP-FPK1 URA3 CEN6*	This study
pKT1638 [pRS416-mRFP1-FPK1]	P_{TPI1}*-mRFP1-FPK1 URA3 CEN6*	This study
pKT1700 [pKO10-GST-FPK1ΔN]	P_{GAL1}*-HA-GST-FPK1ΔN URA3 2 μm*	This study
pKT1702 [pKO10-GST-FPK1(K525R)ΔN]	P_{GAL1}*-HA-GST-FPK1(K525R)ΔN URA3 2 μm*	This study

points, cells were rapidly cooled in an ice bath and analyzed by flow cytometry as described above.

Antibodies

Mouse anti-HA (HA.11) mAb was purchased from BabCO (Richmond, CA). Mouse anti-myc (9E10) mAb was purchased from Sigma. Rabbit anti-Kex2p and anti-Pma1p polyclonal antibodies were gifts from S. Nothwehr (University of Missouri, Columbia, MO) and R. Serrano (Polytechnic University of Valencia, Valencia, Spain), respectively. Mouse anti-Pep12p mAb was a gift from Y. Ohsumi (National Institute for Basic Biology, Okazaki, Japan). For immunoblot analysis, these antibodies were used at the following dilution: anti-HA and anti-myc, 1:1000; anti-Pma1p, 1:5000; anti-Kex2p and anti-Pep12p, 1:2000. Horseradish peroxidase (HRP)-conjugated secondary antibodies (sheep anti-mouse IgG and donkey anti-rabbit IgG) used for immunoblotting were purchased from Amersham Biosciences (Piscataway, NJ).

Sucrose Gradient Fractionation

Fractionation of subcellular organelles based on sedimentation through a sucrose step gradient (Antebi and Fink, 1992) was performed according to procedures described previously (Misu *et al.*, 2003). All fractions were assayed for the relevant distribution of marker proteins by immunoblotting, which was performed as described previously (Misu *et al.*, 2003). SDS-PAGE samples were heated at 37°C for 30 min before loading.

Expression and Purification of the GST-Fpk1p-kinase Domain (GST-Fpk1ΔNp)

The KKT345 (P_{GAL1}*-GST-FPK1ΔN*) strain and the pKT1700 (pKO10-GST-FPK1ΔN) or pKT1702 [pKO10-GST-FPK1(K525R)ΔN] plasmid were constructed to express the C-terminal kinase domain of Fpk1p fused to the C-terminus of GST under the control of the glucose-repressible *GAL1*-promoter. KKT345 cells or KKT268 (*fpk1*Δ *fpk2*Δ) cells harboring pKT1700 or pKT1702 were grown at 30°C to early-logarithmic phase in YPDA (for KKT345) or SDA-U (for KKT268) medium and harvested by centrifugation. The collected cells were resuspended in 1.2 l of YPGA (for KKT345) or SGA-U (for KKT268) medium to a cell density of 0.5 OD_{600}/ml and incubated at 30°C for 12 h. The cells were harvested, washed twice with water, and resuspended in TESD buffer (50 mM Tris-HCl, pH 8.0, 1 mM EDTA, 150 mM NaCl, and 5 mM dithiothreitol) at a volume equal to that of the cell pellet. The cells were lysed with glass beads using Multi-beads shocker (Yasui Kikai Co, Osaka, Japan). After addition of 20 ml of TESD buffer, the cell lysate was centrifuged at 3000 rpm for 5 min at 4°C, and the resulting supernatant was centrifuged at 20,000 × *g* for 30 min at 4°C. Ammonium sulfate was slowly added to the supernatant, and the fraction that precipitated between 40 and 60% (wt/vol) salt saturation was recovered by centrifugation at 20,000 × *g* for 30 min at 4°C. The pellet was dissolved in 20 ml of TESD buffer and loaded onto a glutathione Sepharose 4B column (GE Healthcare, Uppsala, Sweden). The column was washed twice with five bed volumes of TESD buffer and eluted 10 times with one bed volume of TESD buffer containing 10 mM reduced glutathione (Wako Pure Chemicals). A portion of each eluate fraction was subjected to SDS-PAGE, followed by staining with SYPRO ORANGE (Molecular Probes, Eugene, OR). The amount of recovered GST-Fpk1ΔNp was estimated by densitometry with a FLA3000 fluorescent image analyzer (Fuji Photo Film, Tokyo, Japan), using bovine serum albumin as a reference protein. The second eluate fraction, which provided the highest concentration and apparent homogeneity of GST-Fpk1ΔNp (our unpublished results), was used in the phosphorylation assays.

Immunoprecipitation of P-type ATPases and Phosphorylation Assays with GST-Fpk1ΔNp

Immunoprecipitation of P-type ATPases tagged with 13 × myc was performed as described previously (Saito *et al.*, 2004) with the following modifications. Briefly, cells were grown at 30°C to a cell density of 0.5 OD_{600}/ml in YPDA medium. Cells collected from 300 ml (Dnf1p-13myc, Dnf2p-13myc, Drs2p-13myc, and Neo1p-13myc) or 1.2 l (Dnf3p-13myc) of culture were washed twice with ice-cold water and resuspended in 1 ml of lysis buffer (10 mM Tris-HCl, pH 8.0, 300 mM sorbitol, 100 mM NaCl, and 5 mM $MgCl_2$) containing protease inhibitors (1 μg/ml aprotinin, 1 μg/ml leupeptin, 1 μg/ml pepstatin, and 1 mM phenylmethylsulfonyl fluoride). The cells were lysed with glass beads using Multi-beads shocker. Cell lysates were centrifuged at 400 × *g* for 5 min, and the resulting supernatant was centrifuged at 100,000 × *g* for 1 h at 4°C. For immunoprecipitation, pellets were solubilized in 0.45 ml of IP buffer (50 mM Tris-HCl, pH 7.5, 150 mM NaCl, 5 mM EDTA, and 1% 3-[(3-cholamidopropyl) dimethylammonio]-1-propanesulfonate [CHAPS]) containing protease inhibitors. Insoluble material was removed by centrifugation at 20,630 × *g* for 5 min at 4°C. The cleared lysates were incubated with 7.5 μg of anti-myc antibody for 1 h at 4°C. The samples were rotated with 30 μl of protein G-Sepharose 4 Fast Flow (GE Healthcare) for 1 h at 4°C. The protein G-Sepharose beads were pelleted, washed twice with IP buffer, and washed twice with kinase buffer (50 mM Tris-HCl, pH 7.6, 5 mM $MgCl_2$, 1 mM EDTA, and 1 mM EGTA). The beads were equally divided into three tubes. One was subjected to immunoblot analysis with anti-myc antibody (1:1000 dilution), and the others were used for kinase assays. Relative amounts of immunoprecipitated P-type ATPases were estimated by chemiluminescence with a FLA3000 fluorescence image analyzer (Fuji Photo Film).

For kinase assays, beads were suspended in 45 μl of kinase buffer with or without 100 nM purified GST-Fpk1ΔNp. Reactions were started by adding 5 μl of 1 mM [γ-^{32}P]-ATP (2000 cpm/pmol; Perkin Elmer-Cetus, Norwalk, CT; 222 KBq/pmol), followed by incubation at 30°C for 10 min. Reactions were stopped by adding 16.7 μl of 4× SDS-PAGE sample buffer, followed by incubation at 37°C for 30 min. Samples were resolved by SDS-PAGE, and phosphorylated proteins were visualized and ^{32}P incorporation into each P-type ATPase was quantified with a FLA3000 fluorescent image analyzer (Fuji Photo Film).

RESULTS

A Mutation in a Novel Protein Kinase Gene FPK1 Exhibits a Synthetic Lethal Genetic Interaction with the cdc50Δ Mutation

To identify genes involved in *CDC50* and *DRS2* function, we previously screened for mutations that are synthetically lethal with *cdc50*Δ, resulting in isolation of four mutants, each of which harbored an allele of *erg3*, *rgp1*, *vps1*, or *srv2* (Kishimoto *et al.*, 2005). We expanded this screen and isolated alleles of seven genes: *ypt6*, *gsg1/trs85*, *pep8*, *ubp3*, *neo1*, *sec3*,

and *ynr047w*. Ypt6p is a Rab family small GTPase that promotes fusion of recycling endocytic vesicles with the TGN membrane, and Rgp1p is a GDP/GTP exchange factor (GEF) for Ypt6p (Siniossoglou *et al.*, 2000; Siniossoglou and Pelham, 2001). The genetic interaction with *ypt6* and *rgp1* seems to reflect the involvement of Cdc50p-Drs2p in the endocytic recycling pathway (Hua *et al.*, 2002; Saito *et al.*, 2004; Kishimoto *et al.*, 2005; Furuta *et al.*, 2007). Gsg1p/Trs85p is a nonessential subunit of the transport protein complex (TRAPP) II, which is proposed to be a GEF for Ypt31/32p Rab family small GTPases (Morozova *et al.*, 2006). Our recent results showing that the Cdc50p-Drs2p complex interacts with Rcy1p, an effector of Ypt31/32p (Furuta *et al.*, 2007), suggest that TRAPP II is an upstream regulator of Cdc50p-Drs2p. Synthetic lethal interactions with *drs2*Δ were also reported for mutations in other subunits of the TRAPP II complex, *TRS33* and *KRE11* (Sciorra *et al.*, 2005). Pep8p (Vps26p) is a subunit of the retromer, the sorting machinery required for retrieval from the late endosome to the TGN (Seaman *et al.*, 1998; Reddy and Seaman, 2001). Null mutations of *VPS29* and *VPS35*, encoding other retromer subunits, also exhibited synthetic lethality with *cdc50*Δ (our unpublished data), implicating Cdc50p in the late endosome-to-TGN pathway. *NEO1* is the one essential gene among five putative flippases in yeast. Synthetic growth defects of *drs2*Δ and the *neo1-1* temperature-sensitive allele have been reported (Hua and Graham, 2003). Genetic interactions with *ubp3* and *sec3* implicate Cdc50p in unknown functions; Ubp3p is a ubiquitin-specific protease that regulates transport between the ER and Golgi compartments (Cohen *et al.*, 2003), and Sec3p is a spatial landmark that defines sites for polarized secretion (Finger and Novick, 1998). *YNR047W* encodes a novel protein kinase and the results reported herein suggest that Ynr047wp is a regulatory protein kinase for Lem3p-Dnf1p and Lem3p-Dnf2p. We named *YNR047W FPK1* (flippase kinase 1). The synthetic growth defect of the *cdc50*Δ *fpk1*Δ mutants was shown in Figure 1A by tetrad dissection of a sporulated diploid heterozygous for *cdc50*Δ and *fpk1*Δ.

The 893-amino acid Fpk1p contains a C-terminal kinase domain that belongs to the S6 kinase family of serine/threonine kinases (Hunter and Plowman, 1997). Fpk1p has a homolog Kin82p (Ycr091wp). Because the name *KIN82* does not relate to the function of the encoded protein and because we find that Kin82p is functionally related to Fpk1p, we have renamed *KIN82 FPK2*. The kinase domain of Fpk1p is 82% identical and 91% homologous to that of Fpk2p (Figure 1B), whereas the N-terminal domain is 29% identical and 39% homologous (our unpublished results). The kinase domain of Fpk1p is also homologous to proteins from other organisms: NRC-2 (72% identical and 84% homologous) is a negative regulator of the conidiation program in *Neurospora crassa* (Kothe and Free, 1998); phototropin-1 (47% identical and 64% homologous) and phototropin-2 (48% identical and 65% homologous) are blue light–activated protein kinases in *Arabidopsis thaliana* (Briggs and Christie, 2002; Figure 1B).

Single or double knockout of *FPK1* and *FPK2* did not affect cell growth at 18, 30, or 37°C (Figure 1C and our unpublished results). To perform phenotypic analyses of the *cdc50*Δ *fpk1*Δ mutant, we first constructed a conditional mutant in the *fpk1*Δ background in which *CDC50* is expressed under the control of the glucose-repressible *GAL1* promoter. As shown in Figure 1C, the P_{GAL1}-*HA-CDC50 fpk1*Δ mutant grew normally in galactose-containing medium (YPGA), but exhibited only residual growth in glucose-containing medium (YPDA) at 30°C. Deletion of *FPK2* in this strain resulted in a more severe growth defect, whereas the Cdc50p-depleted *fpk2*Δ mutant grew normally (Figure 1C). In addition, the growth defect of the Cdc50p-depleted *fpk1*Δ mutant was suppressed by overexpression of *FPK2* (our unpublished results). These results suggest that Fpk1p and Fpk2p are functionally redundant, but that Fpk1p plays a major role. The *FPK1(K525R)* allele carries an amino acid substitution in the conserved ATP-binding site that results in a kinase-negative mutant protein (Hanks *et al.*, 1988). The Cdc50p-depleted *FPK1(K525R)* mutant also exhibited a growth defect (Figure 1D), suggesting that Fpk1p performs its Cdc50p-related function by phosphorylating target proteins.

*The Cdc50-depleted fpk1*Δ *fpk2*Δ *Mutant Exhibits Defects in the Retrieval Pathway from Early Endosomes to the TGN*

The *lem3*Δ mutation also exhibits synthetic lethality with the *cdc50*Δ and *rcy1*Δ mutations (Saito *et al.*, 2004; Furuta *et al.*, 2007; Supplementary Figure S1). Similarly, the *fpk1*Δ mutation exhibited synthetic lethality with the *drs2*Δ and *rcy1*Δ mutations (our unpublished results); Drs2p is a potential catalytic subunit of Cdc50p (Saito *et al.*, 2004), and Rcy1p is a regulatory factor for the Cdc50p-Drs2p complex (Furuta *et al.*, 2007). These results suggest that Fpk1p/Fpk2p may be functionally related to Lem3p-Dnf1p/Dnf2p. We have recently reported that a temperature-sensitive *cdc50-ts lem3*Δ *crf1*Δ mutant exhibits severe defects in the retrieval pathway from early endosomes to the TGN (Furuta *et al.*, 2007). Thus, we examined this pathway in the Cdc50p-depleted *fpk1*Δ *fpk2*Δ mutant. Tlg1p is a target-SNARE that is recycled between the TGN and early endosomes; GFP-Tlg1p thus shows a punctate pattern reminiscent of endosomal/TGN membranes (Holthuis *et al.*, 1998; Siniossoglou and Pelham, 2001). Snc1p is an exocytic vesicle-SNARE that is recycled from the plasma membrane via early endosomes to the TGN; GFP-Snc1p is primarily localized to the plasma membrane at polarized sites where exocytosis is actively occurring, such as buds (Lewis *et al.*, 2000). Because Tlg1p and Snc1p are both recycled via the retrieval pathway from early endosomes to the TGN, these two proteins accumulate in the same aberrant intracellular structures when this pathway is blocked (Furuta *et al.*, 2007).

Cells expressing mRFP1-Snc1p and GFP-Tlg1p were grown in glucose medium for 6 h. Under these conditions, Cdc50p-depleted cells (P_{GAL1}-*HA-CDC50*) did not exhibit intracellular accumulation of mRFP1-Snc1p, unlike *cdc50*Δ cells (Saito *et al.*, 2004), probably because 6-h incubation was insufficient to completely deplete Cdc50p as described previously (Sakane *et al.*, 2006). Both mRFP1-Snc1p and GFP-Tlg1p were normally localized in wild-type, *lem3*Δ, *fpk1*Δ *fpk2*Δ, and P_{GAL1}-*HA-CDC50* cells (Figure 2A). In contrast, mRFP1-Snc1p and GFP-Tlg1p were colocalized in abnormal membranous structures in the Cdc50p-depleted *fpk1*Δ *fpk2*Δ mutant as well as in the Cdc50p-depleted *lem3*Δ mutant; 92% (n = 105) of the mRFP1-Snc1p–positive structures were also labeled with GFP-Tlg1p in the Cdc50p-depleted *fpk1*Δ *fpk2*Δ mutant (Figure 2A).

The GFP-Snc1p-pm mutant is transported to the plasma membrane by the exocytic pathway but is not internalized by endocytosis (Lewis *et al.*, 2000). GFP-Snc1p-pm was exclusively localized to the plasma membrane in the Cdc50p-depleted *fpk1*Δ *fpk2*Δ mutant as well as in the Cdc50p-depleted *lem3*Δ mutant (Figure 2B). These results are consistent with the notion that intracellular accumulation of mRFP1-Snc1p in the Cdc50p-depleted *fpk1*Δ *fpk2*Δ mutant was due to defects in the retrieval pathway from early endosomes to the TGN, but not due to defects in the exocytic pathway from the TGN.

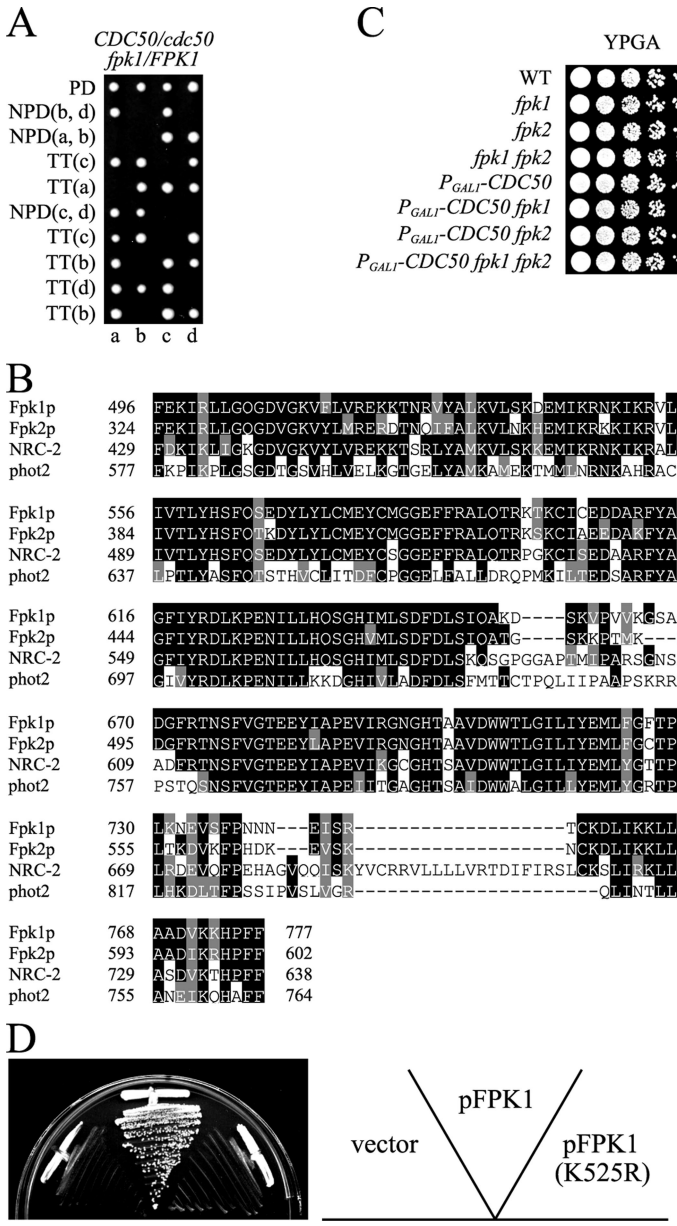

Figure 1. Identification of *fpk1*Δ as a mutation synthetically lethal with the *cdc50*Δ mutation. (A) Tetrad dissection of the *cdc50*Δ*/CDC50 FPK1/fpk1*Δ diploid. Tetrad genotypes (TT, tetratype; PD, parental ditype; and NPD, nonparental ditype) are indicated, and the identities of the double mutant are shown in parentheses. (B) Comparison of the amino acid sequences of Fpk1p, Fpk2p, NRC-2, and phot2 (phototropin-2). The kinase domains were initially aligned using the CLUSTAL W program and the alignment was then optimized by the BOXSHADE program. Black and gray boxes indicate identical and similar amino acids, respectively. The GenBank accession numbers for the given sequences are as follows: *FPK1* (CAA96328.1), *FPK2* (CAA42256.2), NRC-2 (*N. crassa*; EAU37081.1), and phototropin-2 (phot2, *A. thaliana*; AAC27293.2). (C) Growth of the conditional P_{GAL1}-*HA-CDC50 fpk1*Δ *fpk2*Δ mutant. Cells were serially diluted and spotted onto plates containing galactose (YPGA) or glucose (YPDA), followed by incubation at 30°C for 2 d. Strains used were KKT70 (WT, wild type), KKT72 (*fpk1*Δ), KKT266 (*fpk2*Δ), KKT268 (*fpk1*Δ *fpk2*Δ), KKT127 (P_{GAL1}-*CDC50*), KKT117 (P_{GAL1}-*CDC50 fpk1*Δ), KKT331 (P_{GAL1}-*CDC50 fpk2*Δ), and KKT330 (P_{GAL1}-*CDC50 fpk1*Δ *fpk2*Δ). (D) Defective growth of the Cdc50p-depleted *fpk1(K525R)* kinase-negative mutant. KKT117 (P_{GAL1}-*HA-CDC50 fpk1*Δ) harboring YCplac111 (vector), YCplac111-FPK1 (pFPK1), or YCplac111-FPK1(K525R) [pFPK1(K525R)] were grown on a YPDA plate at 30°C for 2 d.

Furuta *et al.* (2007) also reported the mislocalization of C-terminally GFP-tagged Kex2p (Kex2p-GFP) in the *cdc50-ts lem3*Δ *crf1*Δ mutant. Kex2p is a TGN resident furin-like protease that is localized due to constant retrieval from late and early endosomes (Brickner and Fuller, 1997; Lewis *et al.*, 2000). When cycling between endosomes and the TGN is impaired, Kex2p mislocalizes to the vacuole (Wilcox *et al.*, 1992; Spelbrink and Nothwehr, 1999). We examined the localization of Kex2p-GFP in the Cdc50p-depleted *fpk1*Δ *fpk2*Δ mutant and compared it with vacuoles visualized by staining with CellTracker Blue CMAC. In wild-type cells and control mutants, Kex2p-GFP exhibited a punctate pattern reminiscent of TGN membranes, whereas in the Cdc50p-depleted *fpk1*Δ *fpk2*Δ and Cdc50p-depleted *lem3*Δ mutants, Kex2p-GFP was primarily localized to vacuoles with concomitant decrease of the punctate localization (Figure 2C).

In the *cdc50-11 lem3*Δ *crf1*Δ mutant, double membrane structures with ring-, horseshoe-, or crescent-like morphology were accumulated (Furuta *et al.*, 2007). Because Snc1p was localized to these structures by immunoelectron microscopy (Furuta *et al.*, 2007), they seemed to represent the intracellular membranes visualized by light microscopy. We examined membranous structures that accumulated in the Cdc50p-depleted *fpk1*Δ *fpk2*Δ mutant by electron microscopy. When grown in YPDA medium at 30°C for 8 h to deplete Cdc50p, the P_{GAL1}-*HA-CDC50 fpk1*Δ *fpk2*Δ mutant cells accumulated double membrane structures (approximately nine structures [>200 nm in diameter]/10 μm^2; n = 31 sections) to an extent similar to that in the P_{GAL1}-*HA-CDC50 lem3*Δ mutant (~10 structures/10 μm^2, n = 35 sections; Figure 3). The P_{GAL1}-*HA-CDC50* mutant cells accumulated smaller numbers of these structures (approximately four structures/10 μm^2, n = 34 sections; Figure 3). By light microscopy, however, the accumulation of these structures was not apparent (Figure 2A); this difference may be due to longer depletion of Cdc50p (8 h) in the cells used for electron microscopy than in those for light microscopy (6-h deple-

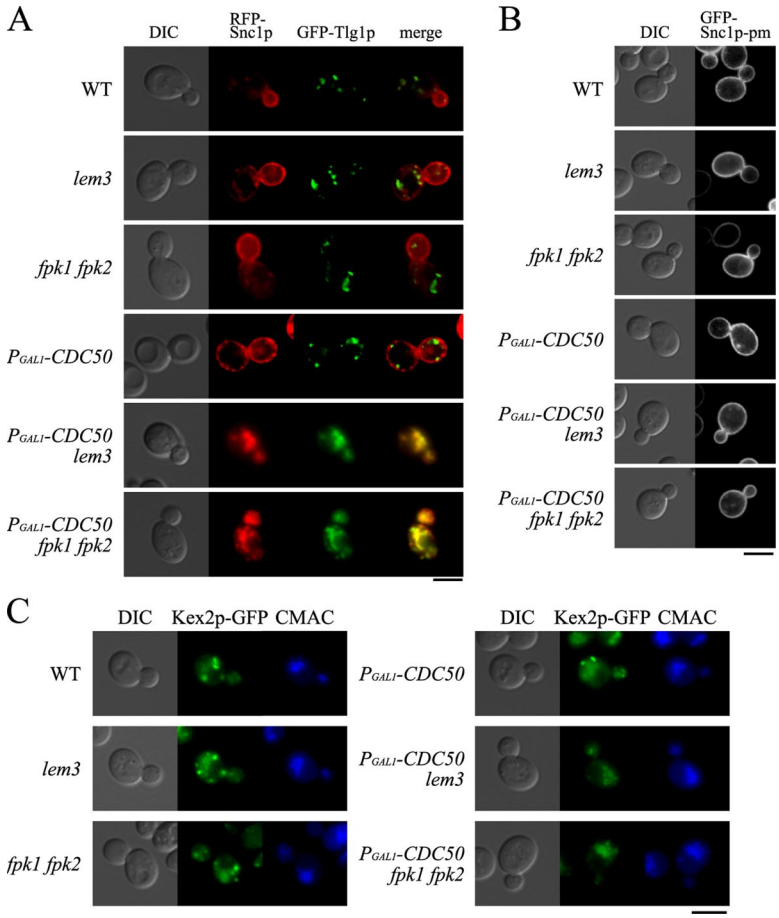

Figure 2. The Cdc50-depleted *fpk1*Δ *fpk2*Δ mutant is defective in vesicle transport from early endosomes to the TGN. (A) mRFP1-Snc1p and GFP-Tlg1p colocalized in abnormal intracellular structures in the Cdc50p-depleted *fpk1*Δ *fpk2*Δ mutant. Cells carrying pKT1566 (YEplac181-GFP-TLG1) and pKT1563 (pRS416-mRFP1-SNC1) were grown at 30°C for 6 h in YPDA medium, followed by microscopic examination after fixation with 0.5% formaldehyde. Strains are those described in the legend for Figure 1C, KKT102 (*lem3*Δ), and KKT293 (P_{GAL1}-*CDC50 lem3*Δ). Images were merged to compare the two signal patterns. (B) GFP-Snc1p-pm localized to the plasma membrane in the Cdc50-depleted *fpk1*Δ *fpk2*Δ mutant. Cells harboring pRS416-GFP-SNC1 pm were grown and examined as described in A. (C) Kex2p-GFP mislocalized to the vacuole in the Cdc50p-depleted *fpk1*Δ *fpk2*Δ mutant. KKT58 (WT), KKT346 (*lem3*Δ), KKT350 (*fpk1*Δ *fpk2*Δ), KKT347 (P_{GAL1}-*CDC50*), KKT348 (P_{GAL1}-*CDC50 lem3*Δ), and KKT349 (P_{GAL1}-*CDC50 fpk1*Δ *fpk2*Δ) cells expressing Kex2p-GFP were grown in YPDA medium at 30°C for 6 h, labeled with CellTracker Blue CMAC at 30°C for 30 min, and observed by fluorescence microscope. Bars, 5 μm.

tion). Abnormal membrane structures were not observed in wild-type, *lem3*Δ, or *fpk1*Δ *fpk2*Δ cells. Taken together, the Cdc50p-depleted *fpk1*Δ *fpk2*Δ and Cdc50p-depleted *lem3*Δ mutants exhibited similar defects in the early endosome-to-TGN transport pathway.

*The fpk1*Δ *fpk2*Δ *Mutant Is Defective in the Inward Translocation of Phospholipids*

Dnf1p and Dnf2p are localized to internal punctate structures reminiscent of endosomal/Golgi compartments and to the plasma membrane at polarized sites (Hua et al., 2002; Pomorski et al., 2003). Lem3p-Dnf1p/Dnf2p and Cdc50p-Drs2p seem to be involved in endocytic recycling as described above (Furuta *et al.*, 2007), whereas Lem3p-Dnf1p/Dnf2p localized at the plasma membrane has been implicated in flipping phospholipids (Kato *et al.*, 2002; Hanson *et al.*, 2003; Pomorski *et al.*, 2003). If Fpk1p and Fpk2p are involved in the function or regulation of Lem3p-Dnf1p/Dnf2p, the *fpk1*Δ *fpk2*Δ mutant might exhibit defects in phospholipid translocation across the plasma membrane.

We thus examined whether the *fpk1*Δ *fpk2*Δ mutations affect the inward translocation of phospholipids at the plasma membrane. If the *fpk1*Δ *fpk2*Δ mutant is defective in flipping phospholipids, a phospholipid enriched in the inner leaflet, such as PE, would be exposed on the outer leaflet of the plasma membrane. Ro09-0198 is a 19-amino acid tetracyclic polypeptide that forms a tight complex with PE in biological membranes (Choung *et al.*, 1988). The *lem3*Δ/*ros3*Δ and *dnf1*Δ *dnf2*Δ mutants exhibited hypersensitive growth to Ro09-0198 (Kato *et al.*, 2002; Pomorski *et al.*, 2003) and to duramycin, an analogue of Ro09-0198 (Noji *et al.*, 2006). Wild-type, *lem3*Δ, *fpk1*Δ, *fpk2*Δ, and *fpk1*Δ *fpk2*Δ strains were grown in YPDA medium containing 5 μM duramycin at 30°C. The *fpk1*Δ *fpk2*Δ mutant showed sensitivity to duramycin, but not to the same extent as the *lem3*Δ mutant (Figure 4A). The kinase-negative *FPK1(K525R) fpk2*Δ mutant also exhibited duramycin sensitivity (our unpublished results). In contrast, neither *cdc50*Δ nor *drs2*Δ mutant exhibited sensitivity to 5 μM duramycin (Supplementary Figure S2).

PE exposed on the outer leaflet of the plasma membrane can be visualized in live cells by staining with biotinylated Ro09-0198 (Bio-Ro; Emoto *et al.*, 1996; Iwamoto *et al.*, 2004). In wild-type cells, PE was exposed at a bud tip during early stages of budding (72% of small-budded cells, n = 103), whereas it was not detected in cells in later budding stages (Figure 4B, WT). In contrast, in *lem3*Δ cells, PE remained exposed at the bud tip throughout the budding process (77% of medium-budded cells, n = 106; 49% of large-budded cells, n = 102), probably due to defective inward translocation of PE (Figure 4B, *lem3*, arrows). Similarly, PE remained exposed in the *fpk1*Δ *fpk2*Δ strain until late stages of budding (40% of medium-budded cells, n = 103; 7% of large-budded cells, n = 107; Figure 4B, *fpk1 fpk2*, arrows). These results suggest that PE is exposed on the outer plasma membrane leaflet in the *fpk1*Δ *fpk2*Δ mutant. Hua *et al.* (2002) reported that the *dnf1*Δ *dnf2*Δ mutant exhibited elongated bud morphology. We confirmed this phenotype in the *lem3*Δ mutant; elongated bud morphology was most prominent in large-budded cells (Figure 4B, *lem3*, large-budded). Interestingly, the *fpk1*Δ *fpk2*Δ mutant also exhibited elongated bud mor-

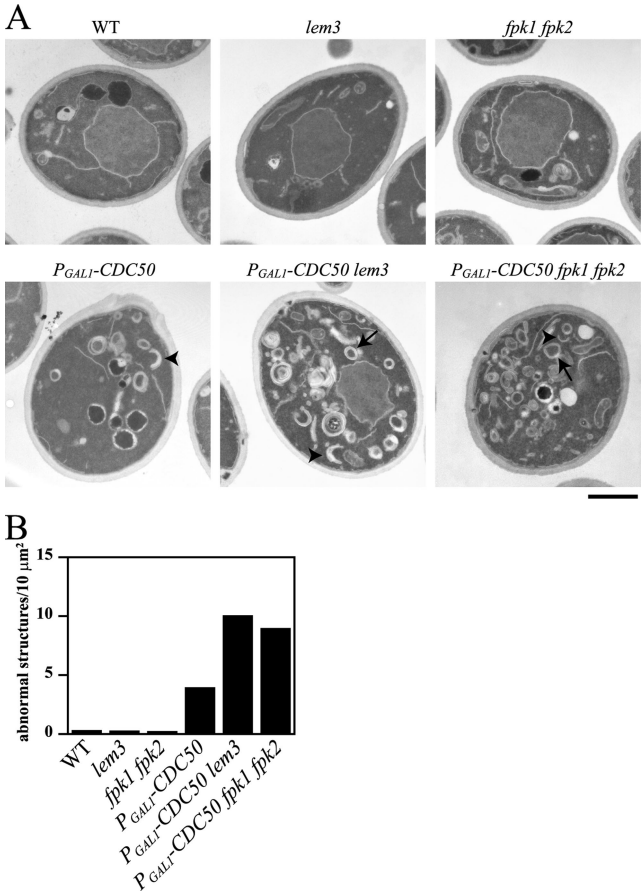

Figure 3. Electron microscopic observation of Cdc50-depleted *fpk1*Δ *fpk2*Δ mutant cells. (A) KKT61 (WT), KKT102 (*lem3*Δ), KKT268 (*fpk1*Δ *fpk2*Δ), KKT287 (P_{GAL1}-*CDC50*), KKT293 (P_{GAL1}-*CDC50 lem3*Δ), and KKT330 (P_{GAL1}-*CDC50 fpk1*Δ *fpk2*Δ) cells were cultured in YPDA at 30°C for 8 h. The cells were fixed with glutaraldehyde-osmium and processed for electron microscopic observation. Arrows and arrowheads indicate representative double-membrane structures with ring- and crescent-shaped morphology, respectively. Bar, 1 μm. (B) Quantitation of abnormal and large (>200 nm in diameter) double membranous structures. Bars represent the number of structures per 10 μm². More than 30 cell sections were examined for each strain.

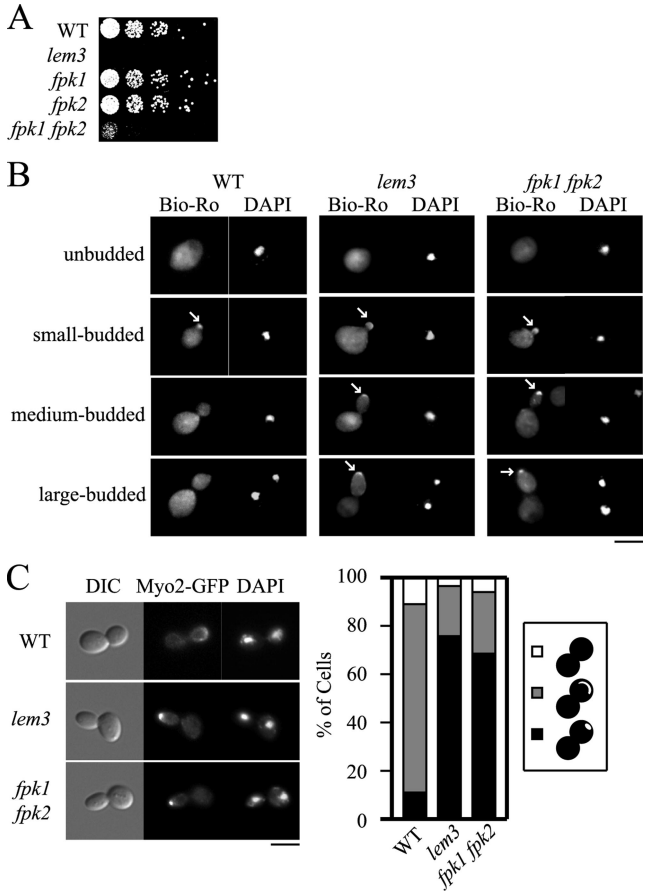

Figure 4. Phosphatidylethanolamine (PE) is exposed on the outer leaflet of the plasma membrane in the *fpk1*Δ *fpk2*Δ mutant. (A) Growth sensitivity of the *fpk1*Δ *fpk2*Δ mutant to duramycin. KKT70 (WT), KKT102 (*lem3*Δ), KKT72 (*fpk1*Δ), KKT266 (*fpk2*Δ), and KKT268 (*fpk1*Δ *fpk2*Δ) strains were cultured in YPDA medium at 30°C, serially diluted, and spotted onto a YPDA plate containing 5 μM duramycin, followed by a 1.5-d incubation at 30°C. (B) PE exposure at the polarized site during bud growth in the *fpk1*Δ *fpk2*Δ mutant. Wild-type (WT), *lem3*Δ, and *fpk1*Δ *fpk2*Δ cells in A were grown to early-midlogarithmic phase, incubated in YPDA medium at 18°C for 3 h, and treated with 100, 30, or 15 μM biotinylated Ro09-0198, respectively, for 13 h (WT and *fpk1*Δ *fpk2*Δ) or 15 min (*lem3*Δ) on ice. After fixation, cells were spheroplasted and incubated with fluorescein streptavidin (Bio-Ro) and DAPI (to distinguish cell cycle stage) as described in *Materials and Methods*. Note that Bio-Ro staining in wild-type cells was observed only in the small-budded stage, whereas staining in *lem3*Δ and *fpk1*Δ *fpk2*Δ cells remained until the large-budded stage (arrows). (C) Localization of Myo2p-GFP in the *fpk1*Δ *fpk2*Δ mutant. KKT75 (WT), KKT351 (*lem3*Δ), and KKT353 (*fpk1*Δ *fpk2*Δ) strains expressing Myo2p-GFP were cultured as in B. Large-budded cells with divided nuclei, recognized by DAPI staining, were categorized as having Myo2p-GFP polarized to the bud tip (black), localized to the bud cortex (gray), and delocalized (white) (n > 100). The bud neck localization pattern, which was excluded from the categorization, was 53.8% (WT), 63.0% (*lem3*Δ), and 49.3% (*fpk1*Δ *fpk2*Δ) in late mitotic cells. A representative cell image is shown in the left panel. Bars, 5 μm.

phology (Figure 4B, *fpk1 fpk2*, large-budded), implying that both Lem3p-Dnf1p/Dnf2p and Fpk1p/Fpk2p are involved in the regulation of bud morphology.

Very recently, we have shown that the elongated bud morphology of the *lem3*Δ mutant is due to defects in the switch from apical to isotropic bud growth (apical-isotropic switch), which is activated by G2 cyclins-Cdc28p (Saito *et al.*, 2007). Lem3p-Dnf1/2p-mediated translocation of phospholipids into the inner leaflet of the apical plasma membrane seems to activate GTPase-activating protein (GAP) activities of Rga1/2p toward the small GTPase Cdc42p, resulting in the dispersal of Cdc42p from the bud tip. In the *lem3*Δ mutant, polarity proteins including a type V myosin Myo2p remained polarized at the bud tip even at a late mitotic phase. We thus examined this phenotype in the *fpk1*Δ *fpk2*Δ mutant. The *fpk1*Δ *fpk2*Δ cells expressing Myo2p-GFP were grown asynchronously, and the localization of Myo2p-GFP was examined in late mitotic cells recognized by DAPI staining. In this analysis, cells with Myo2p-GFP at the bud neck were excluded, because the ratio of the bud neck localization pattern in late mitotic cells was not very different among the stains examined (see the legend to Figure 4C). As shown in Figure 4C, most of the *fpk1*Δ *fpk2*Δ and *lem3*Δ cells exhibited polarization of Myo2p-GFP to the bud tip (68.6 and 75.7%, respectively), whereas only 10.9% of the wild-type cells did. These results indi-

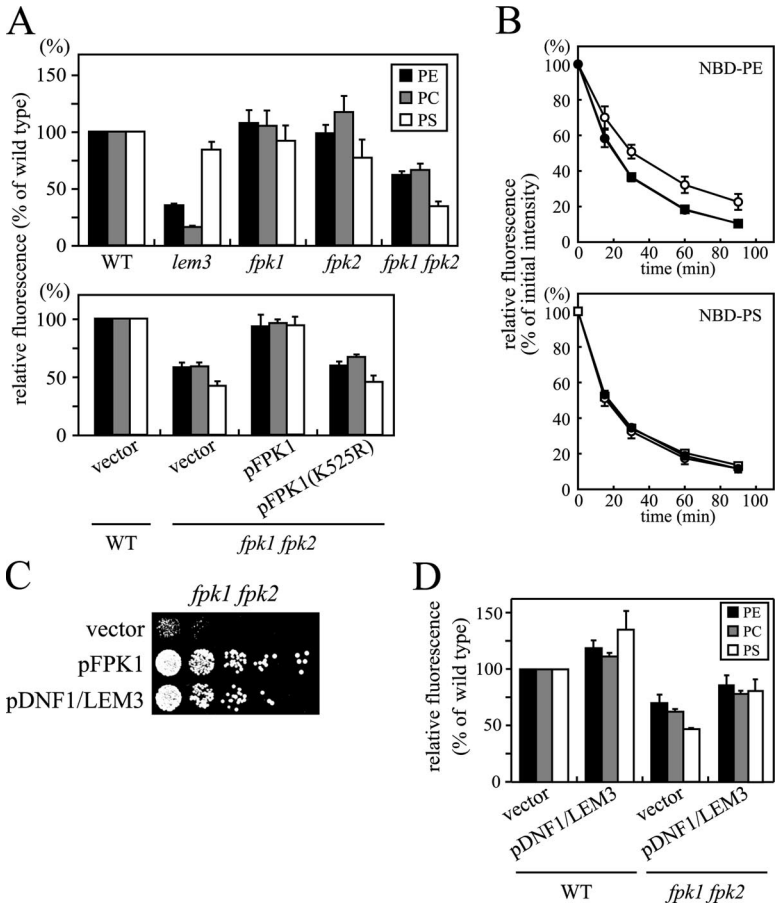

Figure 5. Defective inward translocation of NBD-labeled phospholipids in the *fpk1*Δ *fpk2*Δ mutant. (A) Uptake of NBD-labeled phospholipids. Cells were preincubated in SC medium for 3 h at 30°C and labeled with NBD-PE, -PC, or -PS for 30 min at 30°C, and internalized NBD-phospholipids were quantitated by flow cytometry as described in *Materials and Methods*. Strains used were as follows: top panel, KKT70 (WT), KKT102 (*lem3*Δ), KKT72 (*fpk1*Δ), KKT266 (*fpk2*Δ), and KKT268 (*fpk1*Δ *fpk2*Δ); bottom panel, the wild-type (WT) strain transformed with YCplac111 (vector) and the *fpk1*Δ *fpk2*Δ mutant transformed with YCplac111 (vector), YCplac111-FPK1 (pFPK1), or YCplac111-FPK1(K525R) [pFPK1(K525R)]. Data are presented as average percentage of accumulation relative to wild-type cells ± SD of three independent experiments. (B) Efflux of NBD-PE and NBD-PS was not affected in the *fpk1*Δ *fpk2*Δ mutant. Phospholipid efflux in wild-type (KKT70, ●), *lem3*Δ (KKT102, ○), and *fpk1*Δ *fpk2*Δ (KKT268, □) cells was measured at the indicated times as described in *Materials and Methods*. Relative values for the initial fluorescence in the *lem3*Δ mutant were 91.6 ± 1.3 and 90.5 ± 16.5% of the wild type for NBD-PE and -PS, respectively, and those in the *fpk1*Δ *fpk2*Δ mutant were 96.3 ± 12.4 and 91.2 ± 3.0%, respectively. Data are presented as means ± SD of at least three independent experiments. (C) Simultaneous overexpression of *DNF1* and *LEM3* suppressed the duramycin-sensitive growth of the *fpk1*Δ *fpk2*Δ mutant. *fpk1*Δ *fpk2*Δ cells (KKT268) harboring YEplac181 and YEplac195 (vector), YEplac181 and YEplac195-FPK1 (pFPK1), or YEplac181-LEM3 and YEplac195-DNF1 (pDNF1/LEM3) were tested for duramycin sensitivity as described in the legend of Figure 4A. (D) Simultaneous overexpression of *DNF1* and *LEM3* restored the uptake of NBD-labeled phospholipids in the *fpk1*Δ *fpk2*Δ mutant. Wild-type (WT) and *fpk1*Δ *fpk2*Δ cells harboring YEplac181 and YEplac195 (vector) or YEplac181-LEM3 and YEplac195-DNF1 (pDNF1/LEM3) were assayed for NBD-phospholipid internalization. Results are presented as described in A.

cate that the *fpk1*Δ *fpk2*Δ mutant is also defective in the apical-isotropic growth switch.

We next examined whether the uptake of NBD-labeled phospholipids (NBD-PE, NBD-PC, and NBD-PS) across the plasma membrane was affected in our strains. As described previously, the *lem3*Δ mutant exhibited clear defects in the uptake of NBD-PE (34 ± 1% of wild type) and NBD-PC (16 ± 1% of wild type; Kato *et al.*, 2002; Hanson *et al.*, 2003). In contrast, the uptake of NBD-PS was minimally affected (84 ± 7% of wild type; Figure 5A; Kato *et al.*, 2002; Hanson *et al.*, 2003). Pomorski *et al.* (2003) reported that NBD-PS uptake in *dnf1*Δ *dnf2*Δ cells was ~50% of uptake in wild-type cells; this was also mild compared with the pronounced defects in NBD-PE and -PC uptake. Internalization of NBD-phospholipids was not affected in the *fpk1*Δ or *fpk2*Δ strains, but uptake was significantly decreased in the *fpk1*Δ *fpk2*Δ double deletion strain (62 ± 3% for NBD-PE and 66 ± 5% for NBD-PC relative to wild type; Figure 5A). These results are consistent with weaker sensitivity of the *fpk1*Δ *fpk2*Δ mutant to duramycin. Surprisingly, the uptake of NBD-PS was much more impaired in the *fpk1*Δ *fpk2*Δ mutant (34 ± 4% of wild type) than in the *lem3*Δ mutant. These results raise the interesting possibility that the *fpk1*Δ *fpk2*Δ mutations affect multiple phospholipid translocases. We confirmed that expression of wild-type *FPK1*, but not kinase-negative *FPK1(K525R)*, restored NBD-phospholipid internalization in the *fpk1*Δ *fpk2*Δ mutant (Figure 5A, bottom panel).

Reduced accumulation of NBD-phospholipids in the *fpk1*Δ *fpk2*Δ mutant could be due to increased efflux of NBD-phospholipids rather than decreased internalization. However, the NBD-phospholipid efflux rates measured in the *fpk1*Δ *fpk2*Δ mutant were indistinguishable from those in the wild type for NBD-PE and -PS (Figure 5B). The *lem3*Δ mutant exhibited a little slow efflux of NBD-PE, but the *fpk1*Δ *fpk2*Δ mutant effluxed NBD-PE with a wild-type rate.

Taken together, these results suggest that the reduction in accumulation of NBD phospholipids in the *fpk1*Δ *fpk2*Δ cells is due to a defect in the inward transport of these lipids across the plasma membrane.

One plausible function of Fpk1p/Fpk2p would be the upstream regulation of Lem3p-Dnf1p/Dnf2p. If this were the case, we would expect suppression of the *fpk1*Δ *fpk2*Δ mutations by overexpression of *LEM3* and *DNF1*. The *fpk1*Δ *fpk2*Δ mutant was cotransformed with two multicopy plasmids encoding either *LEM3* or *DNF1*. Simultaneous overexpression of *LEM3* and *DNF1* suppressed the duramycin-sensitive growth of the *fpk1*Δ *fpk2*Δ mutant to an extent similar to that of expression of *FPK1*. The uptake of NBD-PE, -PC, and -PS was also increased in these cells (Figure 5, C and D). Overexpression of *LEM3* and *DNF1* also suppressed the growth defects observed in the Cdc50p-depleted *fpk1*Δ *fpk2*Δ mutant (our unpublished results). In contrast, overexpression of *FPK1* did not suppress the duramycin sensitivity of the *lem3*Δ mutant (our unpublished results). These results are consistent with the hypothesis that Fpk1p/Fpk2p are upstream regulatory kinases of Lem3p-Dnf1p.

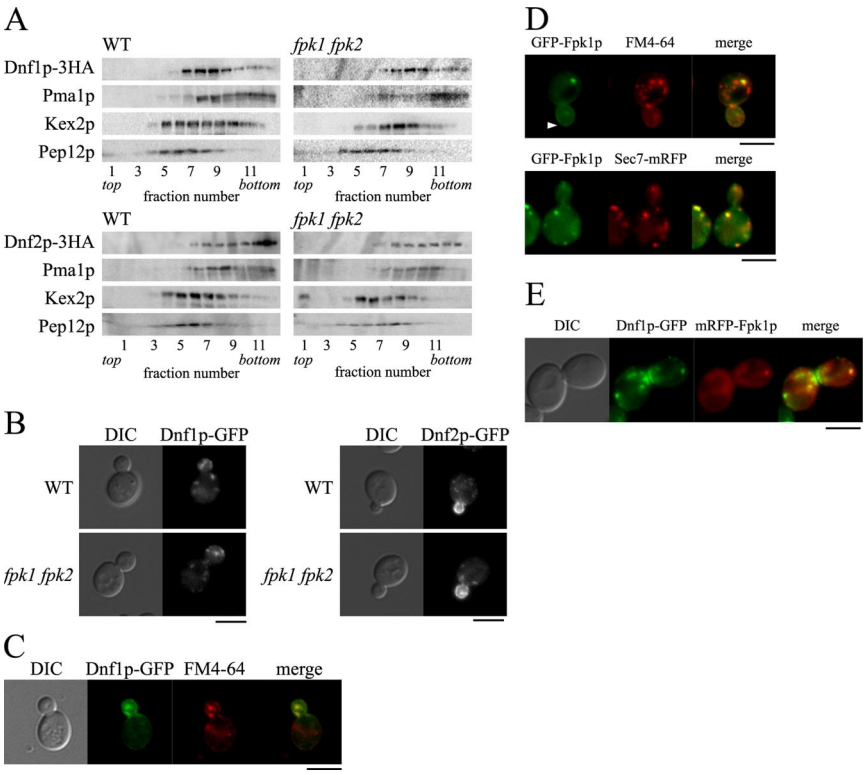

Figure 6. Localization of Dnf1p and Dnf2p is not affected by the *fpk1*Δ *fpk2*Δ mutations. (A) Sucrose gradient centrifugation analysis of Dnf1p-HA and Dnf2p-HA in *fpk1*Δ *fpk2*Δ cells. Cell lysates were prepared from wild-type (WT) and *fpk1*Δ *fpk2*Δ cells expressing either Dnf1p-HA or Dnf2p-HA and fractionated in 18–65% sucrose step density gradients as described in *Materials and Methods*. Equivalent volumes from each fraction were subjected to SDS-PAGE, and proteins were detected by immunoblotting. Strains used were KKT39 (*DNF1-HA*), KKT342 (*DNF2-HA*), KKT340 (*fpk1*Δ *fpk2*Δ *DNF1-HA*), and KKT344 (*fpk1*Δ *fpk2*Δ *DNF2-HA*). (B) Localization of Dnf1p-GFP and Dnf2p-GFP in the *fpk1*Δ *fpk2*Δ mutant. Wild-type (WT) and *fpk1*Δ *fpk2*Δ cells expressing either Dnf1p-GFP (left) or Dnf2p-GFP (right) were grown to early-midlogarithmic phase in YPDA medium at 30°C, followed by fluorescence microscopic observation. Strains used were KKT33 (*DNF1-GFP*), KKT334 (*DNF2-GFP*), KKT332 (*fpk1*Δ *fpk2*Δ *DNF1-GFP*), and KKT336 (*fpk1*Δ *fpk2*Δ *DNF2-GFP*). (C) Punctate structures of Dnf1p-GFP costained with FM4-64. KKT33 (wild type) cells expressing Dnf1p-GFP were incubated with FM4-64 at 30°C for 1 min, followed by fluorescence microscopic observation. (D) Localization of GFP-Fpk1p. GFP-Fpk1p was expressed by transforming cells with the pKT1634 plasmid (pRS416-P_{FPK1}-GFP-FPK1). Cells were grown to early-midlogarithmic phase in SDA-U medium at 30°C, followed by fluorescence microscopic observation. Top, KKT72 (*fpk1*Δ) cells expressing GFP-Fpk1p were labeled with FM4-64 at 30°C for 1 min, and colocalization of GFP-Fpk1p and FM4-64 was examined. Arrowhead indicates the localization of GFP-Fpk1p at the plasma membrane. Bottom, KKT62 (*SEC7-mRFP1*) cells expressing GFP-Fpk1p were examined for colocalization of GFP-Fpk1p with Sec7p-mRFP1. (E) Colocalization of Dnf1p-GFP and mRFP1-Fpk1p. KKT33 (*DNF1-GFP*) cells expressing mRFP1-Fpk1p were examined for colocalization of Dnf1p-GFP with mRFP1-Fpk1p. Cells were grown to early-midlogarithmic phase in SDA-U medium at 30°C, followed by fluorescence microscopic observation. mRFP1-Fpk1p was expressed by transforming cells with the pKT1638 plasmid (pRS416-P_{TPI1}-mRFP1-FPK1). In C–E, images were merged to compare the two signal patterns. Bars, 5 μm.

The Localization of Dnf1p and Dnf2p Is Unaltered in the fpk1Δ fpk2Δ Mutant

Defective inward phospholipid movement across the plasma membrane in the *fpk1*Δ *fpk2*Δ mutant could be due to altered expression or localization of Lem3p-Dnf1p or Lem3p-Dnf2p. Given that Lem3p-Dnf1p is recycled through the endocytic recycling pathway (Saito *et al.*, 2004; Liu *et al.*, 2007), Fpk1p/Fpk2p might regulate localization of Lem3p-Dnf1p/Dnf2p at endosomal compartments or the plasma membrane. To examine these possibilities, we used strains expressing C-terminal GFP- or HA-tagged Dnf1p and Dnf2p from their endogenous loci (Pomorski *et al.*, 2003; Noji *et al.*, 2006). The expression levels of Dnf1p-HA and Dnf2p-HA, as estimated by immunoblotting, were similar in wild-type and *fpk1*Δ *fpk2*Δ strains (our unpublished results).

Localization of Dnf1p-HA and Dnf2p-HA was examined by subcellular fractionation on sucrose density gradients (Figure 6A). In wild-type cells, a plasma membrane marker, Pma1p (a proton ATPase; Serrano *et al.*, 1986; Bagnat *et al.*, 2001), and a late endosome marker, Pep12p (t-SNARE; Becherer *et al.*, 1996; Lewis *et al.*, 2000), were recovered in high- and low-density fractions, respectively. Kex2p, which is localized to endosomal/TGN compartments (Brickner and Fuller, 1997; Lewis *et al.*, 2000), peaked at an intermediate density. Dnf1p-HA peaked at a density similar to that of Kex2p and was distributed into higher densities at which Pma1p fractionated. These results suggest that Dnf1p-HA is primarily localized to endosomal/TGN compartments and is partially localized to the plasma membrane. In contrast, Dnf2p-HA cofractionated with Pma1p, suggesting that it is localized to the plasma membrane. As shown in Figure 6A, the fractionation profiles of Dnf1p-HA and Dnf2p-HA were similar in *fpk1*Δ *fpk2*Δ cells.

We examined the localization of Dnf1p and Dnf2p by microscopic examination of cells expressing GFP-tagged proteins. During most cell cycle stages, Dnf1p-GFP was primarily localized to intracellular punctate structures, which costained with a lipophilic dye, FM4-64, after brief incubation (45.7% of the Dnf1p-GFP dots were merged, n = 127; Figure 6, B and C). It has been suggested that these FM4-64–positive structures are early endosomal/TGN compartments (Lewis *et al.*, 2000; Foote and Nothwehr, 2006), consistent with the results of subcellular fractionation. Similarly, as suggested by the sucrose density fractionation, Dnf2p-GFP localized to polarized plasma membrane sites, such as a bud cortex (Figure 6B). Differential localization of Dnf1p and Dnf2p is consistent with previous observations; the *cdc50*Δ/*drs2*Δ mutations exhibited synthetic growth defects with *dnf1*Δ, but not with *dnf2*Δ (Hua *et al.*, 2002; our unpublished results), whereas defects in NBD-phospholipid internalization were more severe in the *dnf2*Δ mutant (Pomorski *et al.*, 2003; Noji *et al.*, 2006). As shown in Figure 6B, the *fpk1*Δ *fpk2*Δ mutations did not affect localization of Dnf1p-GFP or Dnf2p-GFP. We conclude that the defective phospholipid internalization across the plasma membrane in the *fpk1*Δ *fpk2*Δ mutant was not due to altered intracellular localization of Lem3p-Dnf1p or Lem3p-Dnf2p.

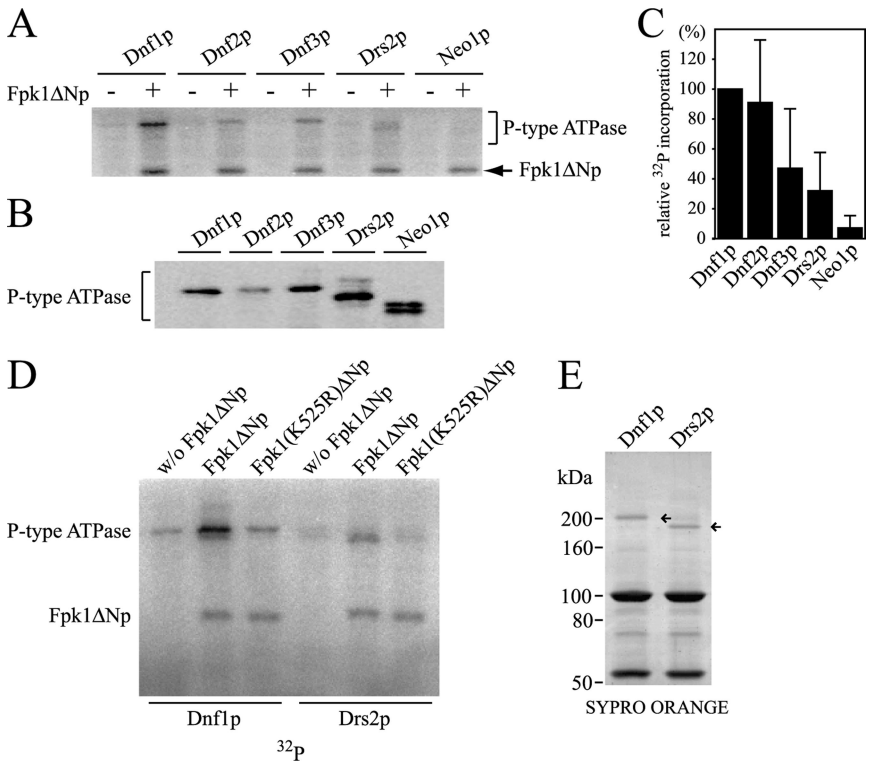

Figure 7. Dnf1p and Dnf2p are phosphorylated by GST-Fpk1ΔNp in vitro. (A) Phosphorylation of P-type ATPases by GST-Fpk1ΔNp. Myc-tagged ATPases were immunoprecipitated from *fpk1*Δ *fpk2*Δ mutant cells and subjected to in vitro kinase assays, as described in *Materials and Methods.* The *fpk1*Δ *fpk2*Δ mutants used were as follows: YKT1363 (*DNF1-myc*), YKT1364 (*DNF2-myc*), YKT1365 (*DNF3-myc*), YKT1366 (*DRS2-myc*), and YKT1367 (*NEO1-myc*). The arrow indicates autophosphorylation of GST-Fpk1ΔNp. (B) Immunoblot of P-type ATPases for quantification. Fractions of the immunoprecipitates in A were subjected to SDS-PAGE, followed by immunoblot analysis using anti-myc antibody. (C) Relative ^{32}P incorporation into P-type ATPases. The extent of ^{32}P incorporation into P-type ATPases was quantified and normalized to the amount of P-type ATPases in immunoprecipitates. ^{32}P incorporation into P-type ATPases in A was measured by a FLA3000 fluorescent image analyzer, and the amounts of immunoprecipitated P-type ATPases in B were estimated by chemiluminescence with a fluorescent image analyzer. The average percentage of phosphorylation relative to Dnf1p is presented ± SD of three (Dnf2p, Dnf3p, and Neo1p) or six (Dnf1p and Drs2p) independent experiments. (D) GST-Fpk1(K525R)ΔNp does not phosphorylate either Dnf1p nor Drs2p. In vitro kinase assays on Dnf1p and Drs2p were performed as described in A with GST-Fpk1ΔNp or GST-Fpk1(K525R)ΔNp, or without GST-Fpk1ΔNp. In these experiments, an equal amount of Dnf1p and Drs2p could be used, as shown in SYPRO ORANGE staining of the SDS-PAGE gel (E, arrows).

Localization of N-terminal GFP-tagged Fpk1p was examined by fluorescence microscopy. *GFP-FPK1* was fully functional, because the Cdc50p-depleted *GFP-FPK1 fpk2*Δ mutant grew normally (our unpublished results). GFP-Fpk1p fluorescence appeared to be distributed throughout the cytoplasm. GFP-Fpk1p was also observed in punctate structures reminiscent of endosomal/TGN compartments in 37.7% of the observed cells (n = 154). In fact, 67.5% of these structures stained with FM4-64 after brief incubation (n = 114) and 62.5% colocalized with the TGN marker Sec7p-mRFP1 (n = 112; Franzusoff *et al.*, 1991; Figure 6D). Furthermore, 64.9% of the mRFP1-Fpk1p punctate structures colocalized with Dnf1p-GFP dots (n = 111; Figure 6E). GFP-Fpk1p was also observed in the plasma membrane, albeit at low frequency (<10% of observed cells; Figure 6D, arrowhead). These results suggest that Fpk1p colocalizes with Dnf1p and Dnf2p at early endosomal/TGN compartments and at the plasma membrane, consistent with the notion that Fpk1p may be a regulatory protein kinase for Dnf1p and Dnf2p.

Phosphorylation of Dnf1p and Dnf2p by GST-Fpk1p In Vitro

We next determined whether purified Fpk1p would phosphorylate immunoprecipitated Dnf1p or Dnf2p in vitro. For this purpose, we expressed the C-terminal fragment of Fpk1p (amino acid residues 445–893) fused to the C-terminus of GST (GST-Fpk1ΔNp) in yeast. GST-Fpk1ΔNp was functional, because P_{GAL1}-*GST-FPK1ΔN drs2*Δ mutant cells grew normally in galactose-containing medium, but not in glucose medium (our unpublished results).

GST-Fpk1ΔNp was purified from yeast cell lysates by glutathione-Sepharose affinity column to apparent homogeneity, as assessed by SDS-PAGE (our unpublished results). Because Fpk1p has been grouped into the S6 kinase family (Hunter and Plowman, 1997), we first assayed GST-Fpk1ΔNp for phosphorylation of the S6 peptide (AKRRRLSSLRA). GST-Fpk1ΔNp phosphorylated the S6 peptide in a dose- and time-dependent manner at 30°C (our unpublished results). We next carried out kinase reactions on immunoprecipitated myc-tagged Dnf1p. Phosphorylated proteins were fractionated by SDS-PAGE, followed by autoradiography. GST-Fpk1ΔNp phosphorylated Dnf1p-myc in a dose-dependent manner (our unpublished results). Immunoblot analysis showed that the immunoprecipitates also contained Lem3p, as previously described (Saito *et al.*, 2004); however, no phosphorylation of Lem3p was observed (our unpublished results), suggesting specific phosphorylation of Dnf1p-myc.

We next determined whether GST-Fpk1ΔNp would phosphorylate Dnf2p, Dnf3p, Drs2p, and Neo1p. The myc-tagged ATPases, including Dnf1p-myc, were immunoprecipitated from cells lacking *FPK1* and *FPK2*, to eliminate possible *FPK1/2*-dependent endogenous phosphorylation. As shown in Figure 7A, in addition to Dnf1p, some extent of phosphorylation was observed for Dnf2p, Dnf3p, and Drs2p, but not for Neo1p. The results also showed that GST-Fpk1ΔNp was autophosphorylated, reminiscent of phototropin autophosphorylation (Briggs *et al.*, 2001). Phosphorylation of the potential noncatalytic subunits of these ATPases, Lem3p (for Dnf2p), Crf1p (for Dnf3p), and Cdc50p (for Drs2p), was not observed (our unpublished results). Because the amount of immunoprecipitated P-type ATPases varied, probably due to differences in expression level and/or protein degradation in cell lysates (Hua *et al.*, 2002; Figure 7B), the extent of ^{32}P incorporation into the P-type ATPases was quantified and normalized to P-type ATPase levels. The results of three

(Dnf2p, Dnf3p, and Neo1p) or six (Dnf1p and Drs2p) independent experiments are shown in Figure 7C. These results indicate that Dnf1p and Dnf2p were most efficiently phosphorylated by GST-Fpk1ΔNp, that Dnf3p and Drs2p were phosphorylated to a lesser extent, and that Neo1p was not phosphorylated.

To exclude a possibility that P-type ATPases were phosphorylated by a nonspecific kinase by which the GST-Fpk1ΔNp preparation was contaminated, we performed the kinase reaction with the kinase-negative GST-Fpk1(K525R)ΔNp. As shown in Figure 7D, Dnf1p and Drs2p were phosphorylated by GST-Fpk1ΔNp, but not by GST-Fpk1(K525R)ΔNp. A minor phosphorylation of Dnf1p observed in the absence of GST-Fpk1ΔNp might be due to a kinase that was present in Dnf1p immunoprecipitates. Autophosphorylation was still observed in GST-Fpk1(K525R)ΔNp, suggesting that the kinase activity of GST-Fpk1(K525R)ΔNp was not completely impaired, possibly due to the substitution to a chemically similar amino acid (Spitaler *et al.*, 2000). In fact, GST-Fpk1(K525R)ΔNp retained 30–40% of the wild-type kinase activity when assayed for the S6 peptide (our unpublished results). Functional deficiency of *FPK1(K525R*) (Figure 1D) seems to be consistent with a notion that the inability of GST-Fpk1(K525R)ΔNp to phosphorylate Dnf1p is physiologically significant. We also wanted to exclude a possibility that GST-Fpk1ΔNp indirectly stimulated phosphorylation of the Aspartate 667, which occurs in the catalytic cycle of P-type ATPases (Bramkamp *et al.*, 2007). The kinase reaction was performed on an immunoprecipitated ATPase-defective mutant Dnf1(D667N)p. Dnf1(D667N)p as well as Dnf1p was phosphorylated by GST- Fpk1ΔNp, but not by GST-Fpk1(K525R)ΔNp (Supplementary Figure S3).

DISCUSSION

The importance of the type 4 subfamily of P-type ATPases (flippases) in cellular function is becoming increasingly appreciated, yet there is much to learn about their regulation. We have recently proposed that Cdc50p-Drs2p is regulated by the Rab family small GTPases Ypt31p/32p and their effector Rcy1p (Furuta *et al.*, 2007). In this study, we report another type of potential regulation: phosphorylation of Dnf1p and Dnf2p by a novel protein kinase Fpk1p. Phenotypic similarities between the *fpk1*Δ *fpk2*Δ and *lem3*Δ mutant strains indicate that Fpk1p/Fpk2p and Lem3p-Dnf1p/Dnf2p function in the same signaling pathway. In the *fpk1*Δ *fpk2*Δ mutant, NBD-phospholipid uptake was impaired, and PE was exposed on the outer plasma membrane leaflet, suggesting that Fpk1p/Fpk2p-dependent phosphorylation is required for Lem3p-Dnf1p/Dnf2p activity. Among the putative flippases in yeast, Dnf1p and Dnf2p were consistently most efficiently phosphorylated by GST-Fpk1p in vitro. Although it should be demonstrated that Dnf1p and Dnf2p are phosphorylated by Fpk1p in vivo also, our results are most consistent with the hypothesis that Fpk1p/Fpk2p are upstream protein kinases for Dnf1p and Dnf2p. No putative flippase has been demonstrated to exhibit phospholipid translocase activity in reconstitution experiments with purified enzyme and chemically defined vesicles. It is possible that activating phosphorylation is required for activity of putative flippases in reconstituted systems.

GST-Fpk1ΔNp also phosphorylated Drs2p and Dnf3p. However, the phenotypes of the *fpk1*Δ *fpk2*Δ mutant may be explained by low Dnf1p and Dnf2p activity. If phosphorylation by Fpk1p plays an important role in regulating both Dnf1p/Dnf2p and Drs2p activity, defects in endocytic recycling would be expected in the *fpk1*Δ *fpk2*Δ mutant. However, the *fpk1*Δ *fpk2*Δ mutant exhibited normal Snc1p localization (Figure 2A). In addition, *fpk1*Δ *fpk2*Δ mutations did not exhibit synthetic lethal interactions with mutations that are synthetically lethal with *cdc50*Δ/*drs2*Δ, including *vps1*Δ (Kishimoto *et al.*, 2005), *vps35*Δ (this study), *pan1-20*, *chc1-5* (Chen *et al.*, 1999), and *arf1*Δ (Chen *et al.*, 1999; Sakane *et al.*, 2006), suggesting that the functions of Cdc50p-Drs2p are not severely impaired in the *fpk1*Δ *fpk2*Δ mutant (our unpublished observations). One possibility is that Cdc50p-Drs2p is regulated by two systems, the Ypt31/32p-Rcy1p and Fpk1p/Fpk2p pathways. In this case, a defect in the Fpk1p/Fpk2p pathway would not cause severe defects in Cdc50p-Drs2p function. In addition, Fpk1p and Fpk2p may be involved in other functions of Drs2p or Dnf3p. For instance, Drs2p has been implicated in clathrin function at the TGN (Chen *et al.*, 1999) and in endocytic internalization at lower temperatures in conjunction with Dnf1p and Dnf2p (Pomorski *et al.*, 2003).

Defects in NBD-PE and -PC uptake as well as growth sensitivity to duramycin were milder in the *fpk1*Δ *fpk2*Δ mutant than the *lem3*Δ mutant, suggesting that the lipid translocase activity of Lem3p-Dnf1p/Dnf2p is not completely abolished in the *fpk1*Δ *fpk2*Δ mutant. In contrast, NBD-PS uptake was severely impaired in the *fpk1*Δ *fpk2*Δ mutant, whereas it was minimally affected in the *lem3*Δ mutant (Figure 5). Because Cdc50p-Drs2p has been implicated in PS translocation (Natarajan *et al.*, 2004) and is recycled through the endocytic-recycling pathway (Saito *et al.*, 2004), it might be that Cdc50p-Drs2p becomes localized to the plasma membrane in the *lem3*Δ mutant to compensate for the loss of PS-translocating activity. However, Cdc50p-GFP was not detected at the plasma membrane in the *lem3*Δ mutant (Saito *et al.*, 2004). Thus, there seems to be an unknown phospholipid translocase that inwardly transports NBD-PS in the *lem3*Δ mutant, and it is an intriguing possibility that Fpk1p/Fpk2p also regulate this lipid translocase. It should be noted that Elvington *et al.* (2005) showed that there are multiple transport pathways for acyl chain–labeled PC analogs; deletion of *LEM3* reduced uptake of NBD-PC and Bodipy FL-PC but had no effect on uptake of Bodipy 581-PC or Bodipy 530-PC. Interestingly, the observation that the *fpk1*Δ *fpk2*Δ mutations exhibit synthetic growth defects with the *lem3*Δ mutation (Supplementary Figure S4) suggests another function of Fpk1p/Fpk2p in addition to the activation of Dnf1p and Dnf2p. In fact, mRFP1-Snc1p was mainly localized to the mother cell plasma membrane in the *fpk1*Δ *fpk2*Δ *lem3*Δ mutant, suggesting that this mutant is defective in endocytosis of Snc1p (our unpublished observations). It is an interesting question whether this defect in endocytosis of Snc1p is related to defects responsible for the loss of NBD-PS uptake in the *fpk1*Δ *fpk2*Δ mutant.

Fpk1p/Fpk2p are involved in endocytic recycling and NBD-phospholipid internalization, indicating that Fpk1p/Fpk2p regulate transbilayer phospholipid movement in two different membranes, early endosomal membranes and the plasma membrane. Are Lem3p-Dnf1p/Dnf2p differently regulated in these two membranes? Because Lem3p-Dnf1p/Dnf2p are recycled through the endocytic recycling pathway (Saito *et al.*, 2004; Liu *et al.*, 2007), complexes activated by Fpk1p/Fpk2p at early endosomes may be still active after they have been transported to the plasma membrane or vice versa. However, Alder-Baerens *et al.* (2006) reported that depletion of Dnf1p and Dnf2p did not affect NBD-phospholipid transport activity on post-Golgi secretory vesicles, suggesting that Lem3p-Dnf1p/Dnf2p on these vesicles are not active. Taken together with our results that GFP-Fpk1p

localized to both early endosomal/TGN membranes and the plasma membrane, it seems that Fpk1p/Fpk2p independently regulate Lem3p-Dnf1p/Dnf2p on these membranes.

Upstream signals that are transmitted via Fpk1p/Fpk2p need to be elucidated in future investigations. Dnf1p and Dnf2p localized at the plasma membrane have been implicated in endocytic uptake of FM4-64 at low temperature (Pomorski *et al.*, 2003), but other functions need to be explored. We have shown that hyperpolarized bud growth in the *fpk1*Δ *fpk2*Δ mutant as well as the *lem3*Δ mutant is caused by defects in a switch from apical to isotropic bud growth that underlies the formation of an ellipsoidal bud shape in budding yeast (Saito *et al.*, 2007; this study). Here, Lem3p-Dnf1p/Dnf2p–mediated transbilayer phospholipid movement at the polarized plasma membrane site seems to trigger down-regulation of Cdc42p through activation of Rga1/2p GAPs, resulting in dispersal of Cdc42p and polarity regulators from the bud tip. Because the apical-isotropic switch is activated by Clb/Cdc28p (Lew and Reed, 1995), Fpk1p/Fpk2p may transduce this signal to Lem3p-Dnf1p/Dnf2p.

An activating signal to Lem3p-Dnf1p/Dnf2p localized at early endosomes may promote endocytic recycling by stimulating vesicle budding from early endosomes. The regulatory signal to Cdc50p-Drs2p may be transmitted via Ypt31/32p and Rcy1p, which interacts with Cdc50p and Drs2p. In contrast, Lem3p-Dnf1p/Dnf2p seem to be differently regulated because neither Dnf1p nor Dnf2p interacts with Rcy1p (Furuta *et al.*, 2007). Efficient endocytic recycling has been implicated in polarized bud growth that is restricted at S and G2 cell cycle phases (Valdez-Taubas and Pelham, 2003); Lem3p-Dnf1p/Dnf2p at early endosomes might also be regulated in a cell cycle–dependent manner.

The kinase domains of NRC-2 and phototropins exhibit sequence homology to Fpk1p, suggesting that these kinases might recognize similar target proteins. NRC-2 was identified as a mutation that constitutively caused conidiation, an asexual developmental program that accompanies changes in cell morphology in the fungus *N. crassa* (Kothe and Free, 1998). Phototropin-1 and -2 are blue-light receptors controlling a range of responses, including phototropism, light-induced stomatal opening, and chloroplast movements, that optimize the photosynthetic efficiency of plants (Christie, 2007). Thus, NRC-2 and phototropins are implicated in membrane-associated functions, and, interestingly, both phototropin-1 and -2 are localized to the plasma membrane (Sakamoto and Briggs, 2002). Downstream targets of NRC-2 and phototropins remain to be identified, but it is noteworthy that phosphorylation of a plasma membrane H^+-ATPase (a type 2 P-type ATPase) is increased when phototropin-1 is autophosphorylated (Kinoshita *et al.*, 2003). It is an interesting possibility that transbilayer changes in phospholipid asymmetry by type 4 P-type ATPases in internal and/or plasma membranes might be involved in downstream functions of NRC-2 and phototropins.

ACKNOWLEDGMENTS

We thank our colleagues in the Tanaka laboratory for valuable discussions. We also thank Eriko Itoh for technical assistance. This work was supported by grants-in-aid for scientific research from the Japan Society for the Promotion of Science and the Ministry of Education, Culture, Sports, Science, and Technology of Japan (T.Y. and K.T.).

REFERENCES

Alder-Baerens, N., Lisman, Q., Luong, L., Pomorski, T., and Holthuis, J. C. (2006). Loss of P4 ATPases Drs2p and Dnf3p disrupts aminophospholipid transport and asymmetry in yeast post-Golgi secretory vesicles. Mol. Biol. Cell *17*, 1632–1642.

Antebi, A., and Fink, G. R. (1992). The yeast Ca^{2+}-ATPase homologue, PMR1, is required for normal Golgi function and localizes in a novel Golgi-like distribution. Mol. Biol. Cell *3*, 633–654.

Aoki, Y., Uenaka, T., Aoki, J., Umeda, M., and Inoue, K. (1994). A novel peptide probe for studying the transbilayer movement of phosphatidylethanolamine. J. Biochem. *116*, 291–297.

Bagnat, M., Chang, A., and Simons, K. (2001). Plasma membrane proton ATPase Pma1p requires raft association for surface delivery in yeast. Mol. Biol. Cell *12*, 4129–4138.

Becherer, K. A., Rieder, S. E., Emr, S. D., and Jones, E. W. (1996). Novel syntaxin homologue, Pep12p, required for the sorting of lumenal hydrolases to the lysosome-like vacuole in yeast. Mol. Biol. Cell *7*, 579–594.

Brachmann, C. B., Davies, A., Cost, G. J., Caputo, E., Li, J., Hieter, P., and Boeke, J. D. (1998). Designer deletion strains derived from *Saccharomyces cerevisiae* S288C: a useful set of strains and plasmids for PCR-mediated gene disruption and other applications. Yeast *14*, 115–132.

Bramkamp, M., Altendorf, K., and Greie, J. C. (2007). Common patterns and unique features of P-type ATPases: a comparative view on the KdpFABC complex from *Escherichia coli.* Mol. Membr. Biol. *24*, 375–386.

Brickner, J. H., and Fuller, R. S. (1997). SOI1 encodes a novel, conserved protein that promotes TGN-endosomal cycling of Kex2p and other membrane proteins by modulating the function of two TGN localization signals. J. Cell Biol. *139*, 23–36.

Briggs, W. R., and Christie, J. M. (2002). Phototropins 1 and 2, versatile plant blue-light receptors. Trends Plant Sci. *7*, 204–210.

Briggs, W. R., Christie, J. M., and Salomon, M. (2001). Phototropins: a new family of flavin-binding blue light receptors in plants. Antioxid. Redox Signal. *3*, 775–788.

Catty, P., de Kerchove, d'Exaerde, A., and Goffeau, A. (1997). The complete inventory of the yeast *Saccharomyces cerevisiae* P-type transport ATPases. FEBS Lett. *409*, 325–332.

Chen, C. Y., Ingram, M. F., Rosal, P. H., and Graham, T. R. (1999). Role for Drs2p, a P-type ATPase and potential aminophospholipid translocase, in yeast late Golgi function. J. Cell Biol. *147*, 1223–1236.

Chen, S. H., Chen, S., Tokarev, A. A., Liu, F., Jedd, G., and Segev, N. (2005). Ypt31/32 GTPases and their novel F-box effector protein Rcy1 regulate protein recycling. Mol. Biol. Cell *16*, 178–192.

Choung, S. Y., Kobayashi, T., Takemoto, K., Ishitsuka, H., and Inoue, K. (1988). Interaction of a cyclic peptide, Ro09-0198, with phosphatidylethanolamine in liposomal membranes. Biochim. Biophys. Acta *940*, 180–187.

Christie, J. M. (2007). Phototropin blue-light receptors. Annu. Rev. Plant Biol. *58*, 21–45.

Cohen, M., Stutz, F., and Dargemont, C. (2003). Deubiquitination, a new player in Golgi to endoplasmic reticulum retrograde transport. J. Biol. Chem. *26*, 51989–51992.

Daleke, D. L. (2007). Phospholipid flippases. J. Biol. Chem. *282*, 821–825.

Devaux, P. F. (1991). Static and dynamic lipid asymmetry in cell membranes. Biochemistry *30*, 1163–1173.

Devaux, P. F., López-Montero, I., and Bryde, S. (2006). Proteins involved in lipid translocation in eukaryotic cells. Chem. Phys. Lipids *141*, 119–132.

Elble, R. (1992). A simple and efficient procedure for transformation of yeasts. Biotechniques *13*, 18–20.

Emoto, K., Kobayashi, T., Yamaji, A., Aizawa, H., Yahara, I., Inoue, K., and Umeda, M. (1996). Redistribution of phosphatidylethanolamine at the cleavage furrow of dividing cells during cytokinesis. Proc. Natl. Acad. Sci. USA *93*, 12867–12872.

Elvington, S. M., Bu, F., and Nichols, J. W. (2005). Fluorescent, acyl chain-labeled phosphatidylcholine analogs reveal novel transport pathways across the plasma membrane of yeast. J. Biol. Chem. *280*, 40957–40964.

Finger, F. P., and Novick, P. (1998). Spatial regulation of exocytosis: lessons from yeast. J. Cell Biol. *142*, 609–612.

Foote, C., and Nothwehr, S. F. (2006). The clathrin adaptor complex 1 directly binds to a sorting signal in Ste13p to reduce the rate of its trafficking to the late endosome of yeast. J. Cell Biol. *173*, 615–626.

Franzusoff, A., Redding, K., Crosby, J., Fuller, R. S., and Schekman, R. (1991). Localization of components involved in protein transport and processing through the yeast Golgi apparatus. J. Cell Biol. *112*, 27–37.

Furuta, N., Fujimura-Kamada, K., Saito, K., Yamamoto, T., and Tanaka, K. (2007). Endocytic recycling in yeast is regulated by putative phospholipid translocases and the Ypt31p/32p-Rcy1p pathway. Mol. Biol. Cell *18*, 295–312.

Gietz, R. D., and Sugino, A. (1988). New yeast-*Escherichia coli* shuttle vectors constructed with *in vitro* mutagenized yeast genes lacking six-base pair restriction sites. Gene *74*, 527–534.

Gietz, R. D., and Woods, R. A. (2002). Transformation of yeast by lithium/acetate/single-stranded carrier DNA/polyethylene glycol method. Methods Enzymol. *350*, 87–96.

Goldstein, A. L., and McCusker, J. H. (1999). Three new dominant drug resistance cassettes for gene disruption in *Saccharomyces cerevisiae*. Yeast *15*, 1541–1553.

Graham, T. R. (2004). Flippases and vesicle-mediated protein transport. Trends Cell Biol. *14*, 670–677.

Guthrie, C., and Fink, G. R. (1991). Guide to Yeast Genetics and Molecular Biology, Methods Enzymol. *194*, Academic Press: San Diego, CA.

Hanks, S. K., Quinn, A. M., and Hunter, T. (1988). The protein kinase family: conserved features and deduced phylogeny of the catalytic domains. Science *241*, 42–52.

Hanson, P. K., Malone, L., Birchmore, J. L., and Nichols, J. W. (2003). Lem3p is essential for the uptake and potency of alkylphosphocholine drugs, edelfosine and miltefosine. J. Biol. Chem. *278*, 36041–36050.

Hanson, P. K., and Nichols, J. W. (2001). Energy-dependent flip of fluorescence-labeled phospholipids is regulated by nutrient starvation and transcription factors, PDR1 and PDR3. J. Biol. Chem. *276*, 9861–9867.

Holthuis, J. C., and Levine, T. P. (2005). Lipid traffic: floppy drives and a superhighway. Nat. Rev. Mol. Cell Biol. *6*, 209–220.

Holthuis, J. C., Nichols, B. J., Dhruvakumar, S., and Pelham, H. R. (1998). Two syntaxin homologues in the TGN/endosomal system of yeast. EMBO J. *17*, 113–126.

Hua, Z., Fatheddin, P., and Graham, T. R. (2002). An essential subfamily of Drs2p-related P-type ATPases is required for protein trafficking between Golgi complex and endosomal/vacuolar system. Mol. Biol. Cell *13*, 3162–3177.

Hua, Z., and Graham, T. R. (2003). Requirement for Neo1p in retrograde transport from the Golgi complex to the endoplasmic reticulum. Mol. Biol. Cell *14*, 4971–4983.

Hunter, T., and Plowman, G. D. (1997). The protein kinases of budding yeast: six score and more. Trends Biochem. Sci. *22*, 18–22.

Iwamoto, K., Kobayashi, S., Fukuda, R., Umeda, M., Kobayashi, T., and Ohta, A. (2004). Local exposure of phosphatidylethanolamine on the yeast plasma membrane is implicated in cell polarity. Genes Cells *9*, 891–903.

Kaplan, J. H. (2002). Biochemistry of Na,K-ATPase. Annu. Rev. Biochem. *71*, 511–535.

Kato, U., Emoto, K., Fredriksson, C., Nakamura, H., Ohta, A., Kobayashi, T., Murakami-Murofushi, K., Kobayashi, T., and Umeda, M. (2002). A. novel membrane protein, Ros3p, is required for phospholipid translocation across the plasma membrane in *Saccharomyces cerevisiae*. J. Biol. Chem. *277*, 37855–37862.

Kikyo, M., Tanaka, K., Kamei, T., Ozaki, K., Fujiwara, T., Inoue, E., Takita, Y., Ohya, Y., and Takai, Y. (1999). An FH domain-containing Bnr1p is a multifunctional protein interacting with a variety of cytoskeletal proteins in *Saccharomyces cerevisiae*. Oncogene *18*, 7046–7054.

Kinoshita, T., Emi, T., Tominaga, M., Sakamoto, K., Shigenaga, A., Doi, M., and Shimazaki, K. (2003). Blue-light- and phosphorylation-dependent binding of a 14–3-3 protein to phototropins in stomatal guard cells of broad bean. Plant Physiol. *133*, 1453–1463.

Kishimoto, T., Yamamoto, T., and Tanaka, K. (2005). Defects in structural integrity of ergosterol and the Cdc50p-Drs2p putative phospholipid translocase cause accumulation of endocytic membranes, onto which actin patches are assembled in yeast. Mol. Biol. Cell *16*, 5592–5609.

Kothe, G. O., and Free, S. J. (1998). The isolation and characterization of *nrc-1* and *nrc-2*, two genes encoding protein kinases that control growth and development in *Neurospora crassa*. Genetics *149*, 117–130.

Lew, D. J., and Reed, S. I. (1995). Cell cycle control of morphogenesis in budding yeast. Curr. Opin. Genet. Dev. *5*, 17–23.

Lewis, M. J., Nichols, B. J., Prescianotto-Baschong, C., Riezman, H., and Pelham, H. R. (2000). Specific retrieval of the exocytic SNARE Snc1p from early yeast endosomes. Mol. Biol. Cell *11*, 23–38.

Liu, K., Hua, Z., Nepute, J. A., and Graham, T. R. (2007). Yeast P4-ATPases Drs2p and Dnf1p are essential cargos of the NPFXD/Sla1p endocytic pathway. Mol. Biol. Cell *18*, 487–500.

Longtine, M. S., McKenzie, A., Demarini, D. J., Shah, N. G., Wach, A., Brachat, A., Philippsen, P., and Pringle, J. R. (1998). Additional modules for versatile and economical PCR-based gene deletion and modification in *Saccharomyces cerevisiae*. Yeast *14*, 953–961.

Misu, K., Fujimura-Kamada, K., Ueda, T., Nakano, A., Katoh, H., and Tanaka, K. (2003). Cdc50p, a conserved endosomal membrane protein, controls polarized growth in *Saccharomyces cerevisiae*. Mol. Biol. Cell *14*, 730–747.

Morozova, N., Liang, Y., Tokarev, A. A., Chen, S. H., Cox, R., Andrejic, J., Lipatova, Z., Sciorra, V. A., Emr, S. D., and Segev, N. (2006). TRAPPII subunits are required for the specificity switch of a Ypt-Rab GEF. Nat. Cell Biol. *8*, 1263–1269.

Natarajan, P., Wang, J., Hua, Z., and Graham, T. R. (2004). Drs2p-coupled aminophospholipid translocase activity in yeast Golgi membranes and relationship to *in vivo* function. Proc. Natl. Acad. Sci. USA *101*, 10614–10619.

Noji, T., Yamamoto, T., Saito, K., Fujimura-Kamada, K., Kondo, S., and Tanaka, K. (2006). Mutational analysis of the Lem3p-Dnf1p putative phospholipid-translocating P-type ATPase reveals novel regulatory roles for Lem3p and a carboxyl-terminal region of Dnf1p independent of the phospholipid-translocating activity of Dnf1p in yeast. Biochem. Biophys. Res. Commun. *344*, 323–331.

Pomorski, T., Holthuis, J. C., Herrmann, A., and van Meer, G. (2004). Tracking down lipid flippases and their biological functions. J. Cell Sci. *117*, 805–813.

Pomorski, T., Hrafnsdóttir, S., Devaux, P. F., and van Meer, G. (2001). Lipid distribution and transport across cellular membranes. Semin. Cell Dev. Biol. *12*, 139–148.

Pomorski, T., Lombardi, R., Riezman, H., Devaux, P. F., van Meer, G., and Holthuis, J. C. (2003). Drs2p-related P-type ATPases Dnf1p and Dnf2p are required for phospholipid translocation across the yeast plasma membrane and serve a role in endocytosis. Mol. Biol. Cell *14*, 1240–1254.

Reddy, J. V., and Seaman, M. N. (2001). Vps26p, a component of retromer, directs the interactions of Vps35p in endosome-to-Golgi retrieval. Mol. Biol. Cell *12*, 3242–3256.

Rose, M. D., Winston, F., and Hieter, P. (1990). Methods in Yeast Genetics: A Laboratory Course Manual, Cold Spring Harbor, NY: Cold Spring Harbor Laboratory Press.

Saito, K., Fujimura-Kamada, K., Furuta, N., Kato, U., Umeda, M., and Tanaka, K. (2004). Cdc50p, a protein required for polarized growth, associates with the Drs2p P-type ATPase implicated in phospholipid translocation in *Saccharomyces cerevisiae*. Mol. Biol. Cell *15*, 3418–3432.

Saito, K., Fujimura-Kamada, K., Hanamatsu, H., Kato, U., Umeda, M., Kozminski, K. G., and Tanaka, K. (2007). Transbilayer phospholipid flipping regulates Cdc42p signaling during polarized cell growth *via* Rga GTPase-activating proteins. Dev. Cell *13*, 743–751.

Sakamoto, K., and Briggs, W. R. (2002). Cellular and subcellular localization of phototropin 1. Plant Cell *14*, 1723–1735.

Sakane, H., Yamamoto, T., and Tanaka, K. (2006). The functional relationship between the Cdc50p-Drs2p putative aminophospholipid translocase and the Arf GAP Gcs1p in vesicle formation in the retrieval pathway from yeast early endosomes to the TGN. Cell Struct. Funct. *31*, 87–108.

Sciorra, V. A., Audhya, A., Parsons, A. B., Segev, N., Boone, C., and Emr, S. D. (2005). Synthetic genetic array analysis of the PtdIns 4-kinase Pik1p identifies components in a Golgi-specific Ypt31/rab-GTPase signaling pathway. Mol. Biol. Cell *16*, 776–793.

Seaman, M. N., McCaffery, J. M., and Emr, S. D. (1998). A membrane coat complex essential for endosome-to-Golgi retrograde transport in yeast. J. Cell Biol. *142*, 665–681.

Serrano, R., Kielland-Brandt, M. C., and Fink, G. R. (1986). Yeast plasma membrane ATPase is essential for growth and has homology with (Na^+ + K^+), K^+- and Ca^{2+}-ATPases. Nature *319*, 689–693.

Siniossoglou, S., Peak-Chew, S. Y., and Pelham, H. R. (2000). Ric1p and Rgp1p form a complex that catalyses nucleotide exchange on Ypt6p. EMBO J. *19*, 4885–4894.

Siniossoglou, S., and Pelham, H. R. (2001). An effector of Ypt6p binds the SNARE Tlg1p and mediates selective fusion of vesicles with late Golgi membranes. EMBO J. *20*, 5991–5998.

Spelbrink, R. G., and Nothwehr, S. F. (1999). The yeast *GRD20* gene is required for protein sorting in the trans-Golgi network/endosomal system and for polarization of the actin cytoskeleton. Mol. Biol. Cell *10*, 4263–4281.

Spitaler, M., Villunger, A., Grunicke, H., and Uberall, F. (2000). Unique structural and functional properties of the ATP-binding domain of atypical protein kinase C-iota. J. Biol. Chem. *275*, 33289–33296.

Valdez-Taubas, J., and Pelham, H. R. (2003). Slow diffusion of proteins in the yeast plasma membrane allows polarity to be maintained by endocytic cycling. Curr. Biol. *13*, 1636–1640.

Wilcox, C. A., Redding, K., Wright, R., and Fuller, R. S. (1992). Mutation of a tyrosine localization signal in the cytosolic tail of yeast Kex2 protease disrupts Golgi retention and results in default transport to the vacuole. Mol. Biol. Cell *3*, 1353–1371.

Zachowski, A. (1993). Phospholipids in animal eukaryotic membranes: transverse asymmetry and movement. Biochem. J. *294*, 1–14.